RESEARCH ON LAND SURFACE PARAMETRIZATION SCHEMES AT ECMWF

C. Blondin
European Centre for Medium-range Weather Forecasts
Reading, U.K.

1. INTRODUCTION

The exchanges of momentum, heat and mass between the atmosphere and the surface are some of the main physical processes that have to be parametrized in numerical models of the atmosphere. Since surface fluxes act as boundary conditions for the atmosphere, the evolution of the atmosphere from a defined initial state becomes more and more dependent on them as time elapses. The actual spatial and temporal distribution of these fluxes contributes to the realisation of the observed climate. This is true over sea and over land, although the processes involved and the time scales are quite different. This paper deals with the formulation of the problem over land.

Many studies have already been devoted to the sensitivity of numerically simulated climates to land-surface conditions (Mintz, 1984). Less work has been published on the sensitivity of the atmosphere to land-surface conditions at shorter time scales. Rowntree and Bolton (1983) demonstrate the impact of persistent soil wetness anomalies on atmospheric moisture fields and surface precipitation within a few days. However, very crude surface schemes were used in most of these studies, the purpose of which was not to question or to assess the schemes themselves. As far as numerical models for weather prediction are concerned, the parametrization of surface fluxes has not been a major concern in the past. Despite this, research activity in this domain has been very active. Very complex schemes are now available (BATS : Dickinson et al., 1986; SiB : Sellers et al., 1986) which emphasize the role of surface processes, especially in relation to the vegetation control of surface fluxes.

In recent years, several weather centres have revised their parametrization of surface fluxes, and now most operational numerical weather prediction models have a rather similar formulation. Most schemes are based on the Monin-Obukhov similarity theory, by computing the turbulent fluxes at the surface, with prognostics equations to simulate the time evolution of soil temperature and wetness in response to the diurnal radiative forcing (Blondin, 1988). The main difference in the surface schemes concerns the formulation of the surface evaporation, and the treatment of snow.

This paper describes how the surface scheme of the ECMWF model has been modified in the last two years. Section 2 describes the evolution of the surface scheme with respect to the incorporation of vegetation. The basis of the design of the scheme is explained. Problems

with the specification of physical characteristics and the initialization of surface variables are illustrated. Results from a priori and a posteriori assessment are compared and discussed. Section 3 deals with the treatment of the snow and its modifications. As in section 2, the physics of the scheme is described and the question of physical characteristics and initialization is addressed. Section 4 summarizes the conclusions that can be drawn after one and a half years of operational forecasts using the schemes presented in sections 2 and 3 and suggests future lines of work.

For convenience, various schemes are referenced using operational model cycle numbers: CY28, CY29 and CY30. They can be interpreted as:

CY28 : old scheme
CY29 : new scheme
CY30 : modified new scheme.

2. EVOLUTION OF THE SURFACE MOISTURE FLUX PARAMETRIZATION

2.1 Brief description of the scheme used up to April 1987 (CY28)

Fig. 1 shows a schematic description of the surface scheme in use up to April 1987. The soil is represented by three layers of respective depths from top to bottom D1 = 0.07 m, D2 = 0.42 m and D3 = D2. The mean temperatures T_s and T_d and wetnesses W_s and W_d of the two uppermost layers (called surface and deep layers) obey the following equations, derived from Budyko (1956) and Deardorff (1978):

$$\frac{\partial T_s}{\partial t} = \frac{F}{C.\,D_1} + 2\,\kappa \frac{(T_d - T_s)}{D_1.(D_1+D_2)} \tag{1}$$

$$\frac{\partial T_d}{\partial t} = 2\,\kappa \frac{(T_s - T_d)}{D_2.\,(D_1+D_2)} + \kappa \frac{(T_{cl} - T_d)}{D_2.D_2} \tag{2}$$

$$\frac{\partial W_s}{\partial t} = \frac{M}{\rho_{H_2O}} + 2\,\lambda \frac{(W_d - W_s)}{D_1.\,(D_1+D_2)} \tag{3}$$

$$\frac{\partial W_d}{\partial t} = 2\,\lambda \frac{(W_s - W_d)}{D_2.(D_1+D_2)} + \lambda \frac{(W_{cl} - W_d)}{D_2.D_2} \tag{4}$$

in which F is the sum of the turbulent (sensible + latent heat) and radiative fluxes (in

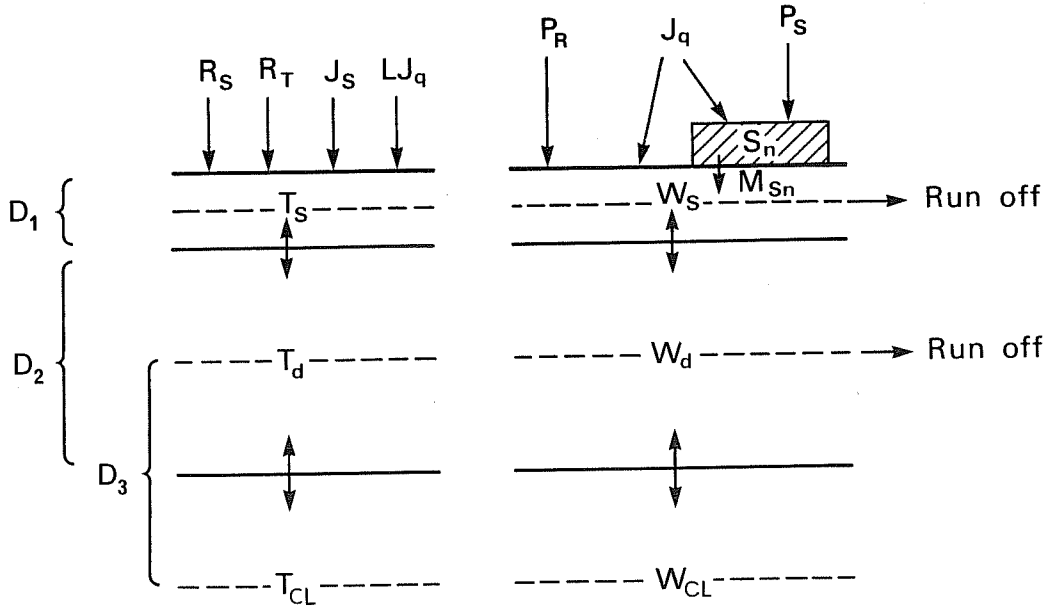

Fig. 1 Schematic representation of the soil parametrization in the ECMWF model (CY28 scheme, see text 2.1).

$W.m^{-2}$), M the sum of the water surface fluxes (precipitation, evaporation, snow melt) (in $kg.m^{-2}$), C the volumetric heat capacity, κ the thermal diffusivity, λ the hydraulic diffusivity and ρ_{H_2O} the density of liquid water, having the values:

$$C = 2.4\ 10^{6}\ J.m^{-3}.K^{-1}$$
$$\kappa = 7.5\ 10^{-7}\ m^{2}.s^{-1}$$
$$\lambda = 1.0\ 10^{-7}\ m^{2}.s^{-1}$$
$$\rho_{H_2O} = 1000\ kg.m^{-3}$$
$$W_{cap} = 0.02\ m$$

When $W_{s'd} > W_{cap}$ (field capacity), the wetness is reset to this maximum value and the difference $(W - W_{cap})$ goes into runoff and is lost to the model.

The sensible heat flux J_s and the evaporation J_q read:

$$J_s = \rho\, C_h \left|U_1\right| (S_1 - S_s) \qquad (5)$$

$$J_q = \rho\, \beta\, C_h \left|U_1\right| [q_1 - q_{sat}(T_s, p_s)] \qquad (6)$$

where the drag coefficient C_h is depending on the surface atmospheric stability (J.F. Louis, 1979; J.F. Louis et al., 1982). Subscripts 1 and s refer to first model level and surface values respectively of dry static energy S, specific humidity q and wind speed U. $q_{sat}(T_s, p_s)$ is the saturation specific humidity at temperature T_s and pressure p_s.

Dew conditions correspond to: $q_{sat}(T_s, p_s) < q_1$

β represents the so-called efficiency of the evapotranspiration. Up to July 1985, the following formula was used:

$$\beta = \beta_0 = C_{Sn} + (1 - C_{Sn}).\ \min\left[1,\ W_s/(0.75.W_{cap})\right] \qquad (7)$$

$$C_{Sn} = \min\left(1,\ Sn/Sn_{cr}\right)$$

in which Sn is the snow depth (in equivalent water depth) and Sn_{cr} is a critical depth ($Sn_{cr} = 0.015$ m).

The formula has been modified in July 1985 to include a temperature dependency:

$$\beta = \beta_0 f(T_S)$$

$$f(T_S) = .75 + .125_* [303\text{-max } \{293, \min (303, T_S)\}] \quad (8)$$

This scheme was not only used in the forecast runs but also in the data assimilation in order to provide estimates of the evaporation rate used to update soil wetnesses on a 6 hour basis (ECMWF, 1984) in combination with precipitation rates derived from surface observations.

Verifications of surface weather elements indicate that in general surface evaporation was overestimated as revealed by too dry initial surface soil wetnesses and too cold forecast surface temperatures, particularly in northern hemisphere mid-latitude summer. There was also spurious precipitation over land which could be interpreted as excessive local recycling of water through surface evaporation.

2.2 Description of the new surface scheme (CY29)

The concept of stomatal resistance (Monteith, 1964) was used to build a parametrization of the evaporation control by vegetation (Blondin, 1986). The final formulation was chosen after some preliminary tests of the sensitivity of T42 90 day runs to various features of the scheme and key parameters describing the soil or the vegetation (results are presented and discussed in 2.3). For practical reasons the number of new geographically variable surface characteristics and time dependent variables was minimized.

Vegetation parameters take the same values at every land grid point, except the vegetation cover which is derived from the Wilson and Henderson-Sellers (1985) dataset. The only new variable is the so-called skin moisture reservoir (cf Eq.19).

The following sub-sections describe the final scheme in some detail. Values of parameters not quoted or relationships not specified indicate that they have been modified since the first operational implementation of the scheme in April 1987 (CY29). The subsequent evolution (CY30) is described in 2.4.

2.2.1 Moisture flux at the surface: Use of somatal resistance and skin reservoir

The first guiding idea is to distinguish between evaporation regimes over bare soils and vegetated areas. C_V being the fractional vegetation cover, the surface moisture flux J_q reads:

$$J_q = C_{Sn} E_{snow} + (1-C_{Sn}) [C_v . E_{vegetation} + (1-C_v) E_{bare})] \quad (9)$$

$$E_{snow} = \rho C_h \left|U_1\right| [q_1 - q_{sat}(T_s, p_s)]$$

Following Monteith, we write:

$$E_{vegetation} = \rho \frac{(q_1 - q_s)}{R_a} = \rho \frac{[q_s - q_{sat}(T_s, p_s)]}{R_c} = \rho \frac{[q_1 - q_{sat}(T_s, p_s)]}{R_a + R_c} \quad (10)$$

where R_a is the aerodynamic resistance, equal to the inverse of the drag, and R_c is the canopy resistance. $R_c$characterizes the physiological control of water loss by the vegetation. (Resistance unit is $s.m^{-1}$).

This canopy resistance depends on many features and can be written in a very general form as:

$$R_c = R_{c0} \cdot g_C \cdot g_{SM} \cdot g_T \cdot g_R \cdot g_D \quad (11)$$

where R_{c0} is a characteristic value, g_C a canopy (seasonal) factor which varies with the phenological state of the plant, g_{SM} a soil moisture stress factor depending on the water availability in the root zone, g_T a temperature stress factor corresponding to the fact that there exists an optimum temperature of life for the plant between some temperature limits, g_R a radiation stress factor since the photosynthesis activity is responsible for the opening of the stomata through which the plant exchanges moisture with the surrounding air and g_D a saturation deficit stress controlling the rate of transfer between the interior of the stomatal cells and the air surrounding the leaves.

In CY29, g_{SM} and g_R are explicitly taken into account (Blondin and Böttger, 1987), but the remaining stress terms are ignored: the temperature and the saturation deficit stresses are very much species dependent and their evaluation requires the knowledge of the leaf temperature and the temperature of the air inside the canopy, both being difficult to diagnose from the single surface temperature T_s. (Opinions about this point have evolved, and this feature of the scheme may well be reconsidered).

The canopy resistance (Sellers, 1985) reads:

$$R_c = R_{c0}\,(PAR)\,.\,[F(w)]^{-1}$$

where:

$$1/R_{c0} = \frac{1}{k.\,c}\left[\frac{b}{d.PAR}\,.\,\ln\left(\frac{de^{k.\,Lt}+1}{d+1}\right) - \ln\left(\frac{d+e^{-k.Lt}}{d+1}\right)\right] \qquad (12)$$

and

$$d = \frac{a+b.\,c}{c.\,PAR} \qquad (13)$$

PAR (Photosynthesis Active Radiation) is taken as 55% of the short wave net radiation flux, while the other parameters have the following values:

$k = 0.9$
$Lt = 4$
$a = 5000\ J.m^{-3}$
$b = 10\ W.m^{-2}$
$c = 100\ s.m^{-1}$

Lt is the leaf area index. The basis of the formula is the assumption that individual leaves having a resistance given by:

$$R_l = \frac{a}{b+PAR} + c \qquad (14)$$

act in parallel. Eq.12 is then the result of a radiation transfer computation in which the variation of PAR within the canopy (due to the interception and shading effect of the leaves) is taken into account.

A clear idea of the actual role of the various coefficients is given by the asymptotic values of R_{c0}:

$$R_{c0}(PAR=\infty) = c / Lt$$
$$R_{c0}(PAR=0) = (a + b.c) / (b.Lt) \sim a / (b.Lt) \qquad (15)$$

c is related to the minimum stomatal resistance, the ratio a/b defining the maximum stomatal resistance.

F(W) reads:

$$F(W) = \begin{cases} 1 & \text{if } W < W_{cr} \\ \dfrac{W - W_{pwp}}{W_{cr} - W_{pwp}} & \text{if } W_{pwp} < W < W_{cr} \\ 0 & \text{if } W < W_{pwp} \end{cases} \qquad (16)$$

where W is now a mean soil wetness in the root zone which can extend through three soil layers, W_{cr} is a critical value above which the evapotranspiration is not affected by the moisture stress and W_{pwp} the so-called permanent wilting point below which it is assumed that the plant is not capable of pumping the water from the root zone to the stomatal cells and thus stops its transpiration.

The root profile is defined by the three quantities R_s, R_d and R_{cl} such that:

$$R_s + R_d + R_{cl} = 1 \qquad (17)$$

so that:

$$W = R_s W_s + R_d W_d + R_{cl} W_{cl} \qquad (18)$$

(The R's are not linear root densities since the W's do not correspond to the same soil depths).

Those relations define the transpiration of the canopy. The evaporation of the canopy is due to the presence of liquid water on the leaves, resulting from precipitation interception and dew collection. This liquid water is assumed to stay in a canopy reservoir which content W_l is thus given by:

$$\frac{\partial W_l}{\partial t} = \frac{e.P_R + E_{skin}}{\rho_{H_2O}} ; \quad W_l \leq W_{lm} \qquad (19)$$

W_{lm} is taken as:

$$W_{lm} = Lt \,.\, W_{lmax} \quad ; \qquad W_{lmax} = 2.10^{-4}\ m \tag{20}$$

$$E_{skin} = \rho\, C_h \left|U_1\right| [q_1 - q_{sat}(T_s, p_s)] \tag{21}$$

and e, the interception efficiency, takes the value 0.25.

The fraction of the canopy which evaporates is given by:

$$C_w = W_l / W_{lm} \tag{22}$$

In the ECMWF surface scheme the use of this reservoir has been extended to accommodate the concept of immediately available water which includes the water stored on the canopy but also the dew deposited on bare soils. Eqs.19 and 20 are thus modified to read:

$$\frac{\partial W_l}{\partial t} = \frac{C_v . e . P_R + E_{skin}}{\rho H_2 O} \tag{23}$$

$$W_{lm} = [C_v . Lt + (1 - C_v)] . W_{lmax} \tag{24}$$

In practice, this modification allows part of the water produced by the surface precipitation and dew to re-evaporate rapidly over the vegetation, but also over bare soil where otherwise it is first diluted in the surface reservoir. This leads to modifying Eq.9 in the form:

$$J_q = C_{Sn} E_{snow} + (1 - C_{Sn}) \{ C_w E_{skin} + (1 - C_w) [C_v E_{vegetation} + (1 - C_v) E_{bare}] \} \tag{25}$$

The evaporation of bare soils is given by:

$$E_{bare} = \rho\, C_h \left|U_1\right| [q_1 - h\, q_{sat}(T_s, p_s)] \tag{26}$$

where h is the relative humidity at the surface depending on W_s only.

2.2.2 Surface hydrology and root uptake

The soil hydrology has also been modified compared to CY28.

W_s and W_d obey the following equations in CY29:

$$\frac{\partial W_s}{\partial t} = \frac{(1-C_{Sn})\,(1-C_w)\,(1-C_v)\,E_{bare}}{\rho H_2 O} + I + 2\lambda \frac{(W_d - W_s)}{D_1 \cdot (D_1 + D_2)} + \gamma + Ext_s \qquad (27)$$

$$\frac{\partial W_d}{\partial t} = 2\lambda \frac{(W_s - W_d)}{D_2 \cdot (D_1 + D_2)} + \lambda \frac{(W_{cl} - W_d)}{D_2 \cdot D_2} + Ext_d \qquad (28)$$

γ is the hydraulic conductivity which takes the value 10^{-10} $m.s^{-1}$ (this value is consistent with the hydraulic diffusivity using Clapp and Hornberger (1978) equations).

The parameter I represents the infiltration of water inside the soil. It is limited by an upper value:

$$I_{max} = 2\lambda \frac{(W_{sat} - W_s)}{D_1 \cdot D_1} + \gamma \qquad (29)$$

where W_{sat} is the soil wetness corresponding to the soil porosity (0.44 m^3/m^3) When the precipitation rate exceeds I_{max}, surface runoff occurs.

In fact surface runoff due to the slope of the terrain inside the grid box is accounted for first. A fraction b of the surface precipitation P_R^* remaining after the canopy interception goes into runoff, where b is given by the empirical formula:

$$b = \frac{\max\,(0,\ V - V_{min})}{V + V_{max}} \qquad (30)$$

where V is the (non-directional) variance of the sub grid scale orography, and:

$$V_{min} = (50)^2\ m^2 \qquad (31)$$

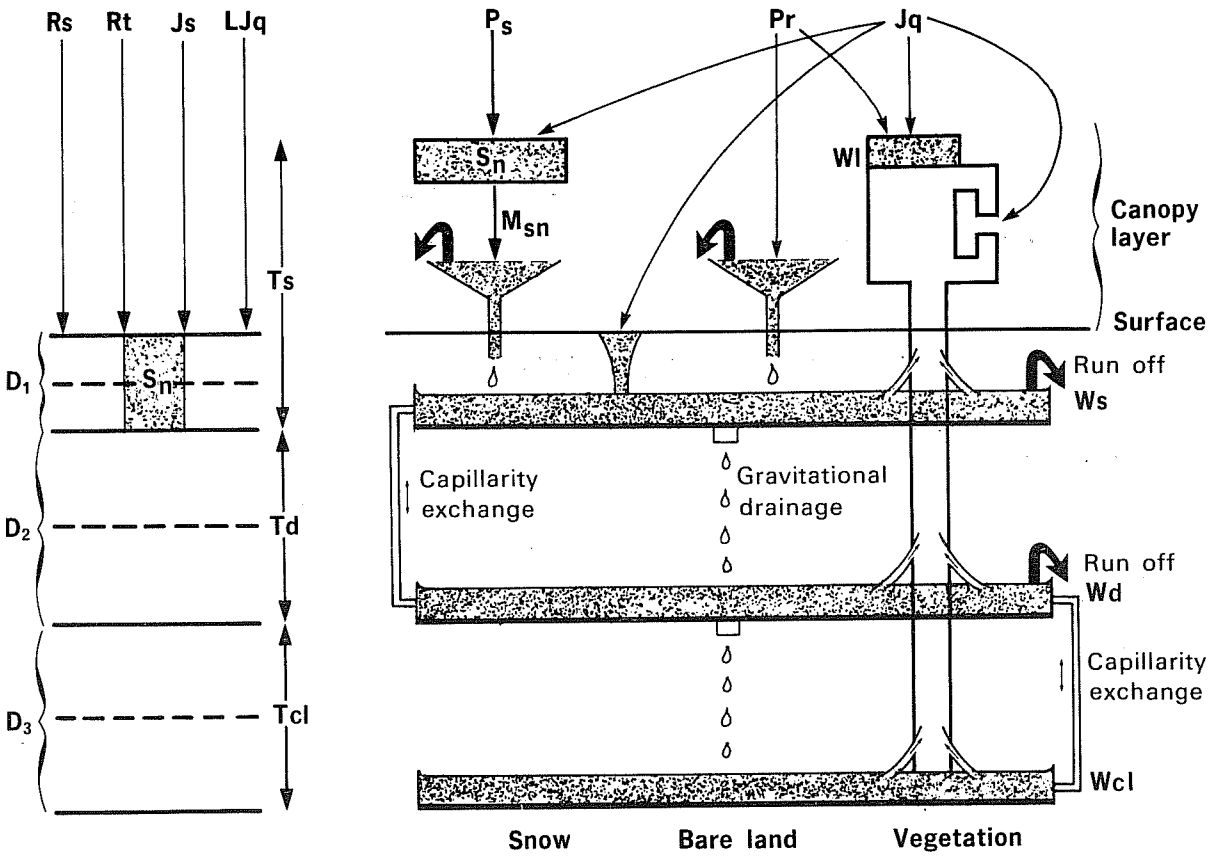

Fig. 2 Schematic representation of the surface and sub-surface parametrization in the ECMWF model (CY29 scheme, see text 2.2).

$$V_{max} = (750)^2\ m^2$$

(In the operational ECMWF model, the largest value of b is 0.5). The fraction (1-b) P_R^* is then compared to I_{max}.

Ext's represent the root uptake in the various reservoirs. The sum of the root uptakes in the reservoirs is assumed to be equal to the canopy transpiration (no water storage in the stems or in the leaves), thus Ext is simply defined by:

$$Ext_{s,d} = \frac{R_{s,d} \cdot W_{s,d}}{\Sigma R_{s,\,d,cl} \cdot W_{s,d,cl}} (1-C_{Sn}) (1-C_w) C_v \frac{E_{vegetation}}{\rho_{H_2O}} \qquad (32)$$

A schematic description of the CY29 scheme is given in Fig.2.

2.2.3 Analysis changes

The other major component of CY29 concerns the revision of the analysis of surface parameters. Because of the failure of the surface soil wetness analysis carried in CY28 to produce satisfactory results, the procedure has been abandoned. In CY29 surface fields produced by the first guess runs of the data assimilation cycles are the initial values for the forecasts. This means that in practice , apart from surface pressure, not a single surface observation enters the analysis of either the atmospheric specific humidity and temperature or the soil wetness and temperature. This solution is temporary and an analysis of surface variables is being developed at ECMWF in the context of a 3-dimensional variational analysis. However, the use of such a procedure for a long time is a very severe test for the scheme and should give valuable input for the design of an improved surface scheme in terms of selection of parameters, physical processes to be represented and use of observations. Examples of the feedback of operational assessment onto some aspects of the surface parametrization are given in 2.4

2.3 Elements of comparison of CY28 and CY29

The results presented in this section have been obtained with the CY29 scheme in which h and R's are given by:

$$h = 1 - \cos\left(\frac{\pi}{2} \cdot \frac{W_s}{W_{cap}}\right) \qquad (33)$$

$$R_s = 0.02;\ R_d = 0.49;\ R_{cl} = 0.49 \qquad (34)$$

2.3.1 One dimensional simulation of the sensitivity of the diurnal cycle of surface variables to changes of the surface scheme

The direct impact of the differences between CY28 and CY29 is illustrated qualitatively in Figs.3.

Both surface schemes are used to simulate the diurnal evolution of a column of soil in response to an imposed atmospheric forcing. The time evolution of wind, air temperature and humidity is prescribed, as well as the net short wave and the downward long wave radiation flux at the surface. Typical mid-latitude summer conditions are simulated. The soil temperatures in the three soil layers are set equal to the air temperature at the first model level at sunset. The three soil reservoir contents are initialized at half the field capacity. Precipitation amounts are forced each afternoon to simulate the possible convective activity for the time of the year. The differences between the two schemes are clear. During daytime, the sensible heat flux (J_s) is larger with CY29 than with CY28 while the opposite is observed for the latent heat flux ($L.J_q$); the surface temperature (T_s) is higher with CY29. On average, the upper reservoir content (W_s) decreases with CY28 but increases with CY29, indicating that the water needed for the surface moisture flux does not come mainly from this reservoir due to the root vertical distribution in CY29.

Of interest is the correlation between the precipitation and the time evolution of the surface variables. Since the evaporation efficiency depends on W_s only in CY28, (cf Eqs. 6 and 7) precipitation has a negligible impact on both the surface fluxes and the surface temperature. Only the upper surface reservoir reacts to the income of water. The behaviour of CY29 is very different. The interception of the rain by the canopy causes a rapid increase of the canopy evaporation, reducing the sensible heat flux and the surface temperature at the same time. The upper reservoir captures the infiltrated water, but this water can be used efficiently to feed the transpiration only when it enters the intermediate reservoir. Thus, the surface moisture flux increases in the CY29 run, but at a lower rate than it decreases in CY28 in response to the surface soil layer moisture depletion.

The results of this simple experiment also explain why the CY28 scheme leads to overestimated evaporation rates. The β coefficient was appropriate when no diurnal cycle was simulated in the atmospheric model. The drag coefficient C_h and the β coefficient fluctuated on comparable time scales. If a diurnal cycle is included, daytime values of C_h representative of a generally unstable turbulent surface layer become large, whilst β cannot decrease accordingly because daily variations of W_s are small. (In the ECMWF model, Ws represent the moisture content of 7 cm of soil).

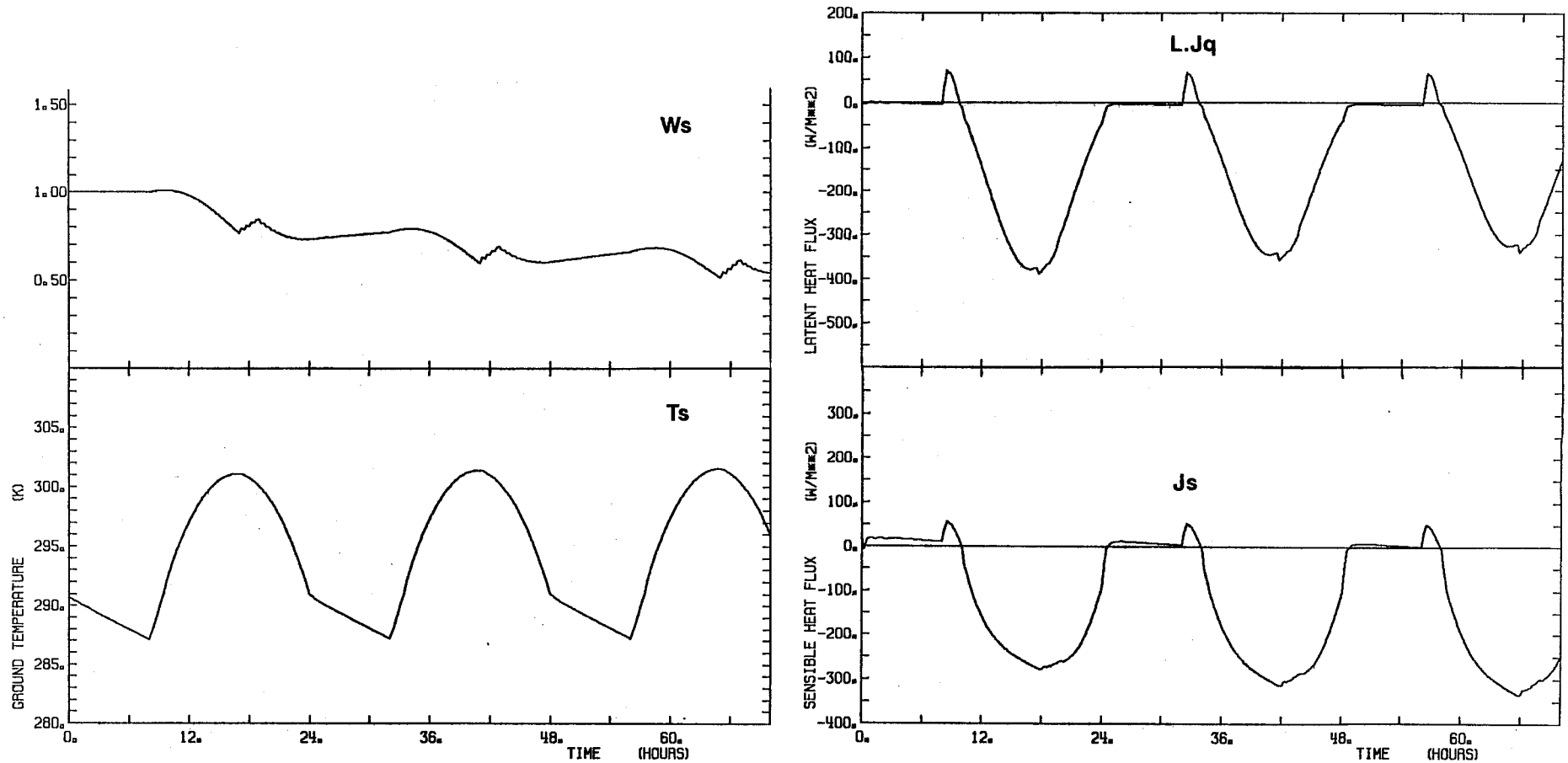

Fig. 3 a) Simulation of the diurnal cycle of surface variables and fluxes using the CY28 scheme (cf text 2.3.1).

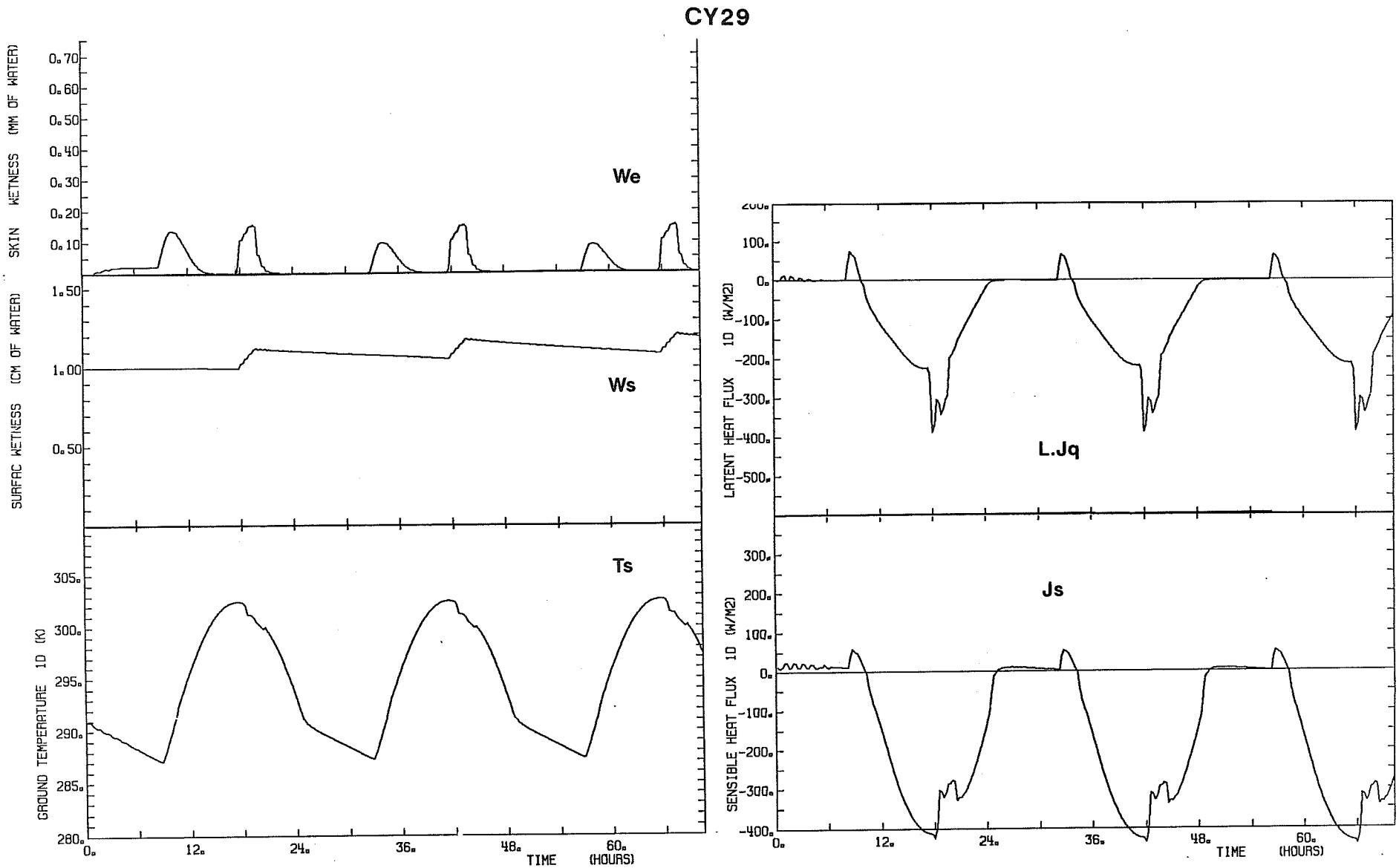

Fig. 3 b) Same as 3a, but for CY29.

2.3.2 Sensitivity of the model climate

In order to study the sensitivity of the model climate to the parametrization of land-surface processes, a T42 version of the model has been run for two periods of 90 days representative of winter and summer conditions of each hemisphere. Initial conditions for the upper air fields correspond to a mean state obtained by averaging December and January analyses on one hand and June and July on the other hand, whilst the surface variables (temperature and moisture in the various model slabs below the surface) were set at their climate values for 15 January and 15 June respectively. During the course of the runs, sea surface temperatures and soil temperatures and wetnesses of the deepest layer are updated on a five day basis and set at their climate value for the current date. An estimate of the yearly mean simulated climate is obtained by averaging results of two 90 day runs for the two different periods.

The impact on global and annual average energy fluxes into and out of the atmosphere is illustrated on Fig.4, which contains as a reference an estimate of those quantities by Verstraete and Dickinson (1986), referred to as V and D later. The Bowen ratio over the continents is too small in CY28 runs (0.5 as opposed to 0.86 from V and D). CY29 runs improves on this (0.64), which shows the role of the stomatal resistance in controlling surface evaporation. In parallel, higher surface sensible heat and long wave radiation fluxes are obtained over the continents.

Convective activity is directly affected by the change of the surface scheme. Both the surface convective precipitation and the amount of convective clouds are reduced over the land areas in the CY29 runs. Fig.5 indicates that in the summer northern hemisphere, on average deep convective clouds do not develop as high in CY29 as in CY28 runs. The occurrence of convective events is also reduced. The effect on the tropospheric circulation of using different surface parametrizations is rather weak as judged from looking at 90 day mean 850 and 200 hPa velocity potential and stream function fields. However, in relation to the decrease of convective activity in the tropics, a weakening of the Hadley circulation is noticeable. The export of heat towards extratropical regions is achieved directly by a more active large eddy circulation.

The impact on the surface variables themselves is summarized in Table 1. The variations in the heat budget of the ground correlate with the variations of the surface heat fluxes: less evaporation induces higher surface temperatures and more sensible heat is transferred into the atmosphere. The variation of the temperature of the intermediate reservoir of the winter northern hemisphere runs is connected to the revision of the soil thermal properties for snow covered grounds (this illustrates the impact of the modifications described in 3.1 for the treatment of snow).

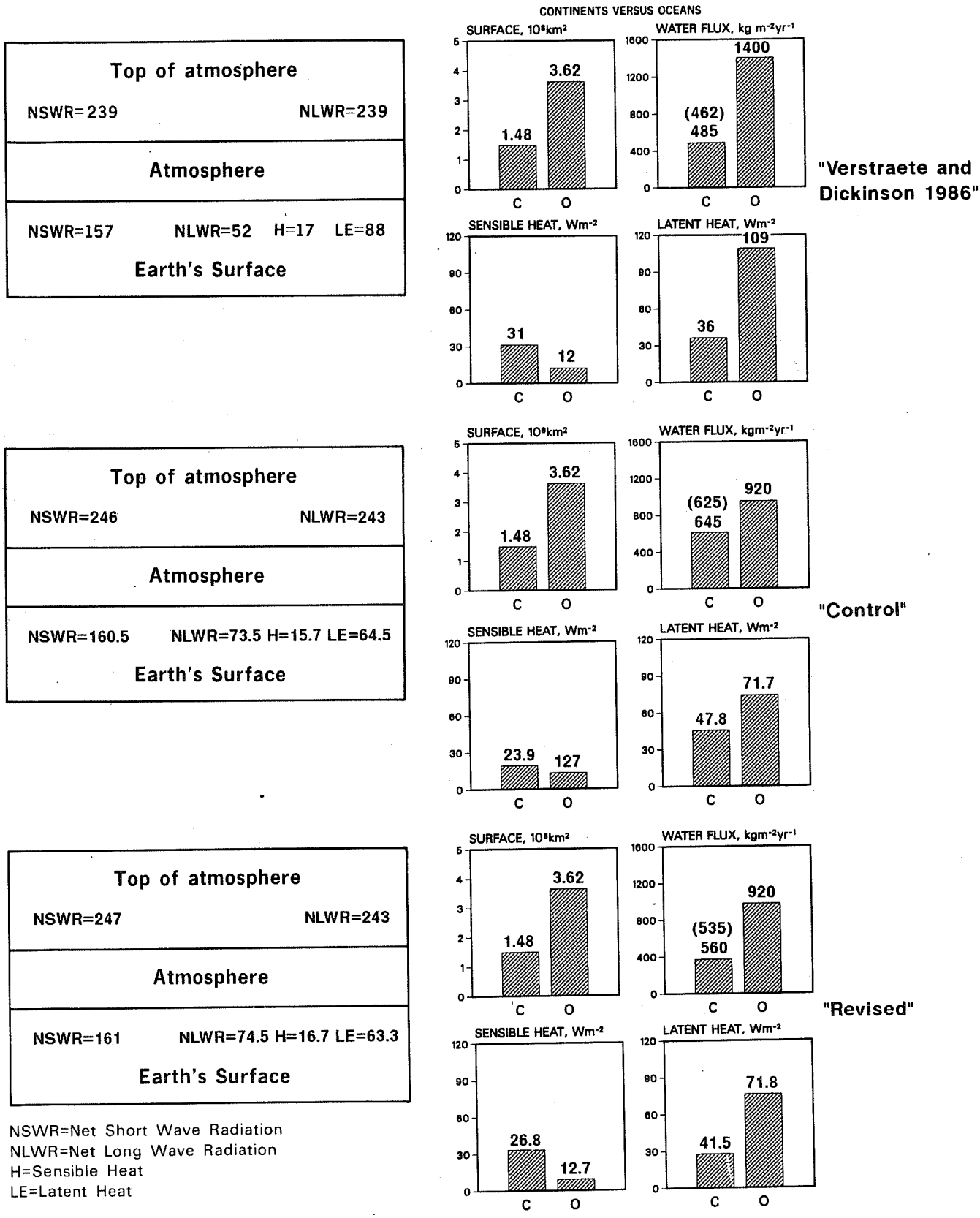

Fig. 4 Left hand side: Global and annual average energy fluxes into and out of the atmosphere, in $W.m^{-2}$.
Right hand side: Comparison between oceans and continents, in terms of area, evaporation, sensible and latent heat annual mean fluxes.

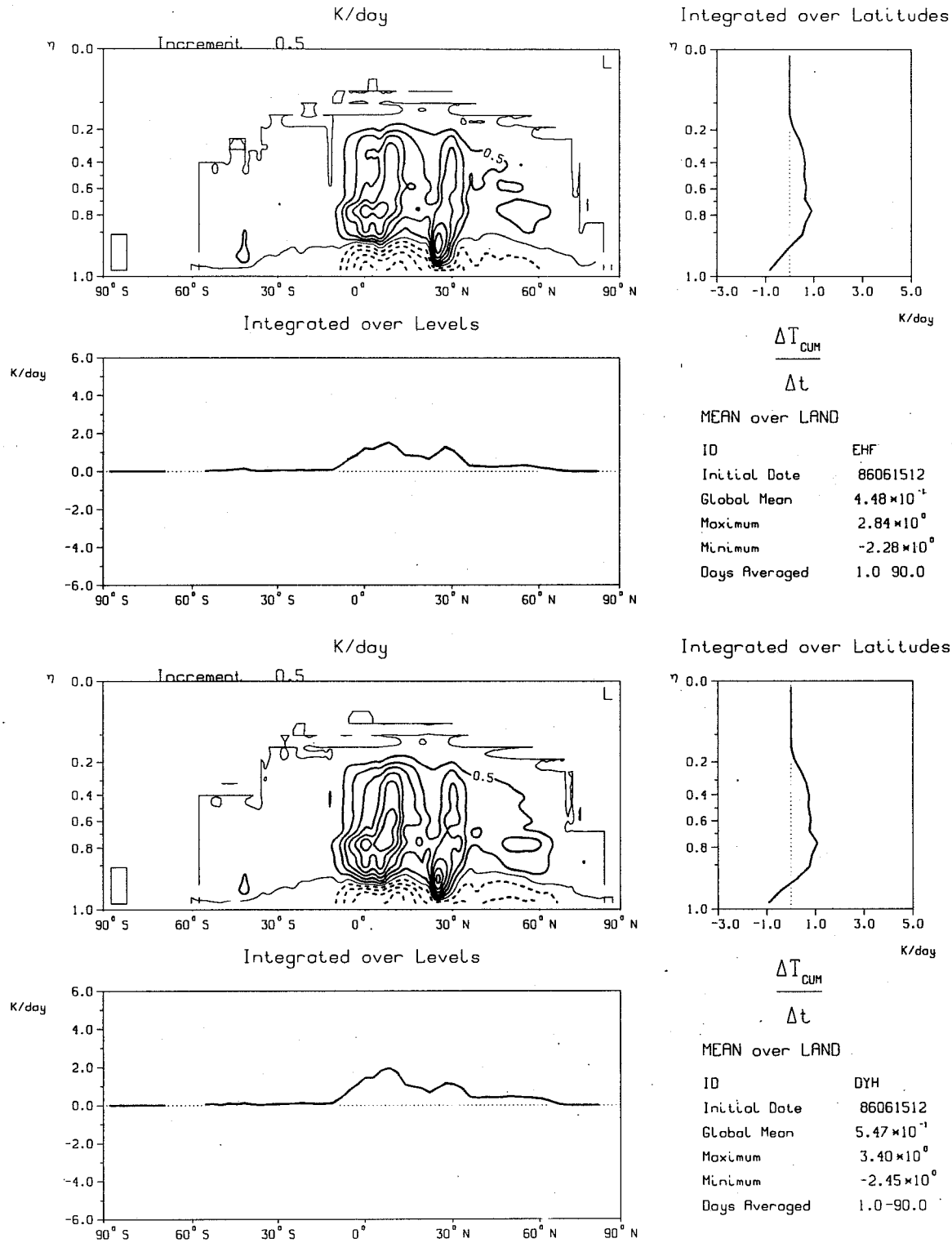

Fig. 5 90 day averaged zonal mean tendency over land of the temperature T due to deep convection using CY28 (bottom) and CY29 (top) surface schemes.

Table 1

	T_s (°C)	T_d (°C)	H($W.m^{-2}$)	LE($W.m^{-2}$)	W_s (cm)	W_d (cm)	E/P_R
WINTER NORTHERN HEMISPHERE							
CY28	1.31	1.90	17.1	40.8	1.14	1.18	0.68
CY29	1.35	2.31	18.8	36.1	1.25	1.20	0.65
SUMMER NORTHERN HEMISPHERE							
CY28	12.2	11.5	30.7	54.8	0.877	0.929	0.80
CY29	12.4	11.7	34.8	46.8	1.08	0.974	0.78

90 day mean surface variables and fluxes for all the land grid points and for the run representative of the wintertime of the northern hemisphere (upper part) and the one of the summertime of the northern hemisphere (lower part).

Table 1 shows how the moisture content in the soil is affected by the modifications in the parametrization of land-surface processes. On average less evaporation leads to more storage of water in the reservoirs. Nevertheless the various final states are obtained via rather different moisture transfers at the surface and in the ground. Water extraction by the root system in the intermediate reservoir induces a strong convergence of water in this reservoir in the CY29 runs. Also the decrease of the ratio Evaporation/Precipitation corresponds to the increase of the surface run-off which is due mainly to the surface runoff on sloping terrain (Eq.30).

Five sensitivity experiments have also been carried out with the CY29 scheme (T42 runs of two periods of 90 days as already described).

Only one feature of the CY29 scheme is changed at a time. The experiments correspond to the following modifications:

- LR (for Low Resistance): in Eq. 12, $c = 25\ s.m^{-1}$
- HR (for High Resistance): in Eq. 12, $c = 1000\ s.m^{-1}$

- RO (for ROot): in Eq. 32, $R_s = 1.$, $R_d = R_{cl} = 0.$ (all the roots are in the upper reservoir);

- NS (for No Skin reservoir): $W_{lmax} = 0.$ (no interception of precipitation by the vegetation and the dew enters into the ground);

- VG (for VeGetation): $C_v = 1$ for all land points.

As mentioned when comparing the CY28 and CY29 runs, there is , on average, little sensitivity of the mean tropospheric flow to somehow moderate changes in the surface fluxes over the continents.

Results are summarized in Table 2.

Table 2

	T_s (°C)	T_d (°C)	H($W.m^{-2}$)	LE($W.m^{-2}$)	W_s (cm)	W_d (cm)	E/P_R
WINTER NORTHERN HEMISPHERE							
CY29	1.35	2.31	18.8	36.1	1.25	1.20	0.65
LR	1.02	2.15	18.5	37.2	1.26	1.19	0.67
HR	1.91	2.67	20.1	32.5	1.24	1.21	0.60
RO	1.32	2.30	20.9	33.7	1.20	1.21	0.65
NS	1.52	2.47	20.6	32.4	1.23	1.17	0.61
VG	1.54	2.40	20.8	34.8	1.29	1.21	0.63
SUMMER NORTHERN HEMISPHERE							
CY29	12.4	11.7	34.8	46.8	1.08	0.974	0.78
LR	12.2	11.6	34.2	48.3	1.08	0.967	0.77
HR	13.4	12.3	36.7	39.3	1.05	0.986	0.72
RO	12.6	11.8	37.6	42.6	0.973	0.985	0.75
NS	12.9	12.1	37.1	41.3	1.04	0.931	0.72
VG	12.6	11.9	36.1	45.5	1.12	0.984	0.75

90 day mean surface variables and fluxes for all the land grid points and for the run representative of the wintertime of the northern hemisphere (upper part) and the one of the summertime of the northern hemisphere (lower part).

The impact of the variation of the stomatal resistance is straightforward: the higher the resistance, the smaller the evaporation and the higher the sensible heat flux and the soil

temperatures. A large value of the resistance favours also a larger storage of water in the ground (since D2 = 6.D1, W_d has to be multiplied by 6 to be compared with W_s in terms of actual amount of water). However the upper reservoir contains less water if the canopy has a higher stomatal resistance which suggests that bare lands have to contribute more to compensate for the reduction of moisture flux over the vegetation.

The RO experiment shows that when all the roots are concentrated in the surface reservoir, W_s, E and E/P_R decrease but that W_d increases slightly. This means that the moisture diffusion inside the ground, which is a process of a longer time scale than the evaporation, cannot supply enough water to maintain the moisture flux at its value when roots directly extract water from the deeper layer. This result depends strongly on the way climate values are used to update the deepest layer variables. It gives however the indication that the fewer roots in the "climate" reservoir, the less evaporation.

The results of the NS run highlight the efficiency and the importance of accounting for the interception of precipitation by the canopy layer. To suppress this process has approximately the same effect as multiplying the stomatal resistance by a factor of 10 as in HR. The decrease in the E/Pr corresponds to an increase of surface runoff since total precipitation enters the infiltration test and the runoff calculation due to sloping terrain rather than this amount minus the intercepted water. Note that as in the RO run, despite lower values of the surface temperature, the sensible heat flux is larger than in the HR run (to a lesser extent, the same is true for the VG run).

The assumption that the continents are entirely covered by some vegetation leads to modest changes. Clearly the storage of water in the ground becomes more important (see W_s,W_d and E/P_R for the VG run). Otherwise this seems to be the modification to which the model is the least sensitive. This is because the actual vegetation cover is strongly connected to the average value of the soil wetness. This is also the case in the model though soil climate values and vegetation cover have been obtained using completely independent datasets. To put vegetation over desert areas without modifying the soil climate at the same time does not allow for important changes in the surface fluxes.

It can be said that on average the model soil variables and the surface fluxes evolve in a rather predictable way when the parametrization of the land surface processes is modified. However there are some aspects of these results which are far less clear and may be characteristic of the ECMWF model.

First the role of the heat flux inside the ground which is partly determined by the climate values used in the deepest reservoir is far from negligible since it accounts for approximately $10.Wm^{-2}$ in the balance at the surface.

Secondly, in Table 2, which summarizes the results for the continents, it is remarkable that the sum $J_s+L.J_q$ almost shows the same variations as $L.J_q$. The net radiation at the surface behaves in the same way but with variations of less amplitude. This suggests a non trivial interaction with the radiation through the cloud field. It might have been reasonable to assume that any modification of the surface scheme leading to a direct reduction of the surface evaporation should induce a reduction of the cloudiness, leading to a larger net radiation flux at the ground. A possible equilibrium then corresponds to higher surface temperatures, larger sensible heat fluxes and smaller latent heat fluxes despite the increase of the potential evapotranspiration, thus leading to higher $J_s+L.J_q$.

Other diagnostics indicate that the effect upon convective and low clouds is to reduce their amount because of less convective activity and drier boundary layers, but that mid-tropospheric cloud amount varies in the opposite way. As shown in Fig. 4, the reduction of moisture flux over the continents is partly balanced by an increase over the oceans. This may be sufficient to drive a slightly more humid mid-tropospheric flow over most of the continents. Obviously the combined effect of the modification of the surface fluxes and of the cloud forcing may lead to only subtle changes in the mean tropospheric flow which are simply not detectable with the rather crude analysis which has been performed.

These results give valuable information on the possible impact of the change of surface schemes on model climate. The mean variations of surface variables and fluxes must also be found both in the data assimilation through the first guess runs and in the 10 day forecasts. However, the actual impact is more difficult to quantify. It is known that surface fluxes increase with model resolution because of more variability in the atmospheric flow. For instance the underestimation of the surface evaporation over the oceans obtained in T42 runs as apparent in Fig.4 may not be as large at the operational T106 resolution. A recent study by S. Esbensen indicates that the model predicted surface fluxes over the oceans are quite close to the best possible estimates (S. Esbensen, personal communication).

The next sub-section presents results obtained with the CY29 scheme used at T106 resolution.

2.3.3 Impact in operational forecasts

Two operational forecasting suites, using CY28 and CY29 schemes, have been run in parallel between 01/04/87 and 06/04/87.

The synoptic forecasts look very similar during the whole period as far as geopotential or atmospheric temperature are concerned. However the surface fluxes and the surface variables exhibit significant differences over the continents, in qualitative agreement with results presented in 2.3.2. On average for the continents, the soil wetness in the upper reservoir is larger in the CY29 suite, showing much more consistency during the course of forecasts than in the CY28 suite. This mainly comes from a clear bias of the analysed soil wetness in regions of sparse data coverage and convective precipitation towards too small values when the CY28 surface analysis is performed.

Information concerning the surface fluxes over the continents is summarized in Table 3.

Table 3

	10 day mean sensible heat flux ($W.m^{-2}$)	10 day mean latent heat flux ($W.m^{-2}$)	10 day mean convective precipitation (mm/day)	10 day mean large scale precipitation (mm/day)
CY28	29	46	1.33	0.72
CY29	34	38	1.22	0.69

Mean 10 day surface fluxes averaged over the 6 10 day forecasts run in parallel between the 01 and the 06/04/87

As in the climate sensitivity runs, it can be noticed that the decrease of the latent heat flux from CY28 to CY29 (8 $W.m^{-2}$) does not balance the increase of sensible heat flux (5 $W.m^{-2}$). Therefore $J_s+L.J_q$ also decreases. The convective precipitation is clearly much more affected than the large scale one, indicating the strong link between local evaporation and convection. Most of the reduction of the surface convective precipitation occurs in the equatorial regions, but large variations can be observed, ranging from a decrease of more than 8.5 mm/day to an increase of almost 7 mm/day.

A much clearer picture of the effect of the change was obtained after a few months of use of the CY29 scheme. Fig. 6 shows the 10 day mean of the sensible heat flux averaged for the period 15/07 to 31/08 1986 (Fig.6 a) and 1987 (Fig.6 b). Figs.7 and 8 represent the

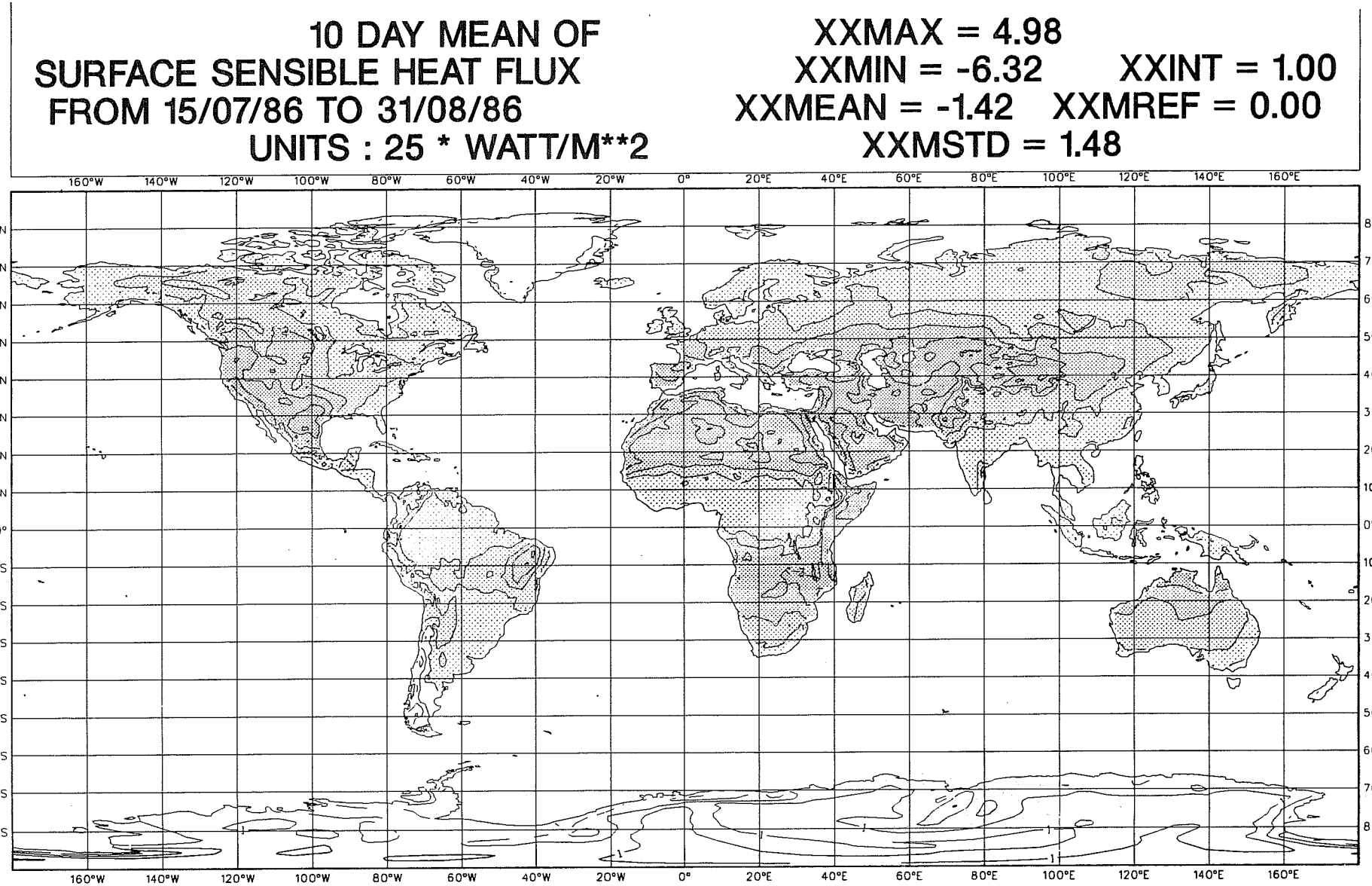

Fig. 6 a) 10 day mean of surface sensible heat flux over the continents for all forecasts from 15/07/86 to 31/08/86 (CY28 scheme used).

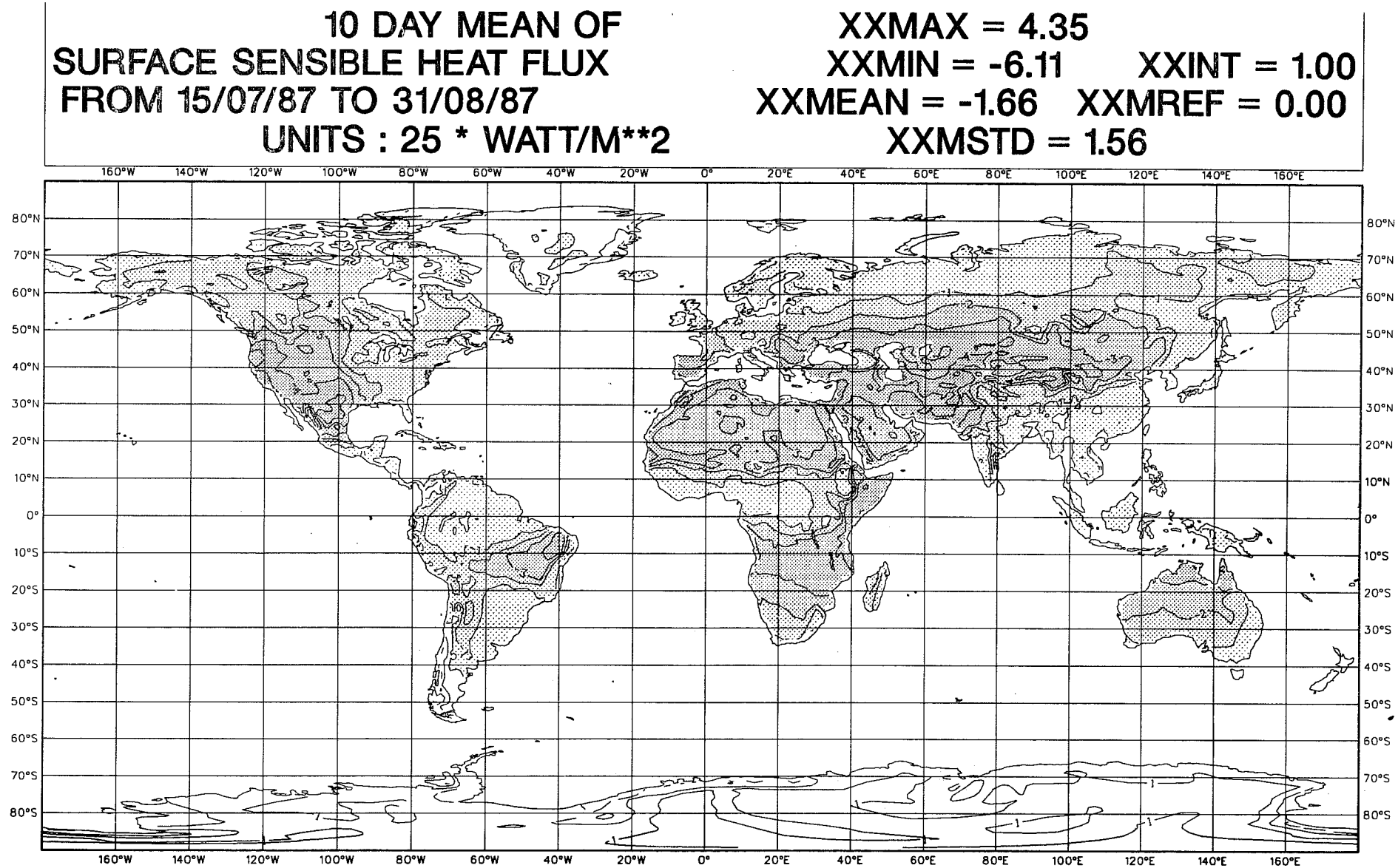

Fig. 6 b) Same as Fig. 6a) but for the period 15/07/87 to 31/08/87 (CY29 scheme used).

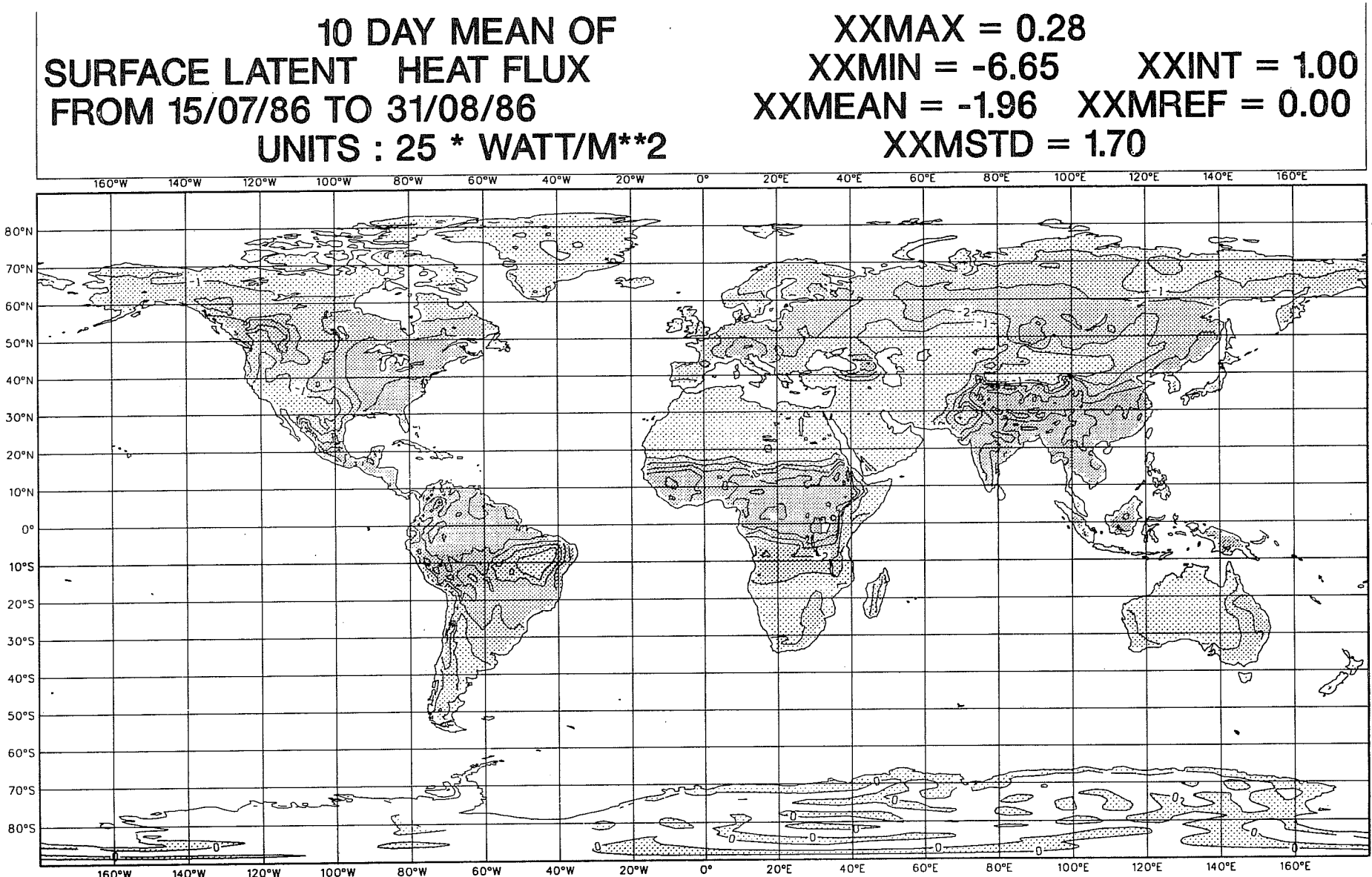

Fig. 7 a) 10 day mean of surface latent heat flux over the continents for all forecasts from 15/07/86 to 31/08/86 (CY28 scheme used).

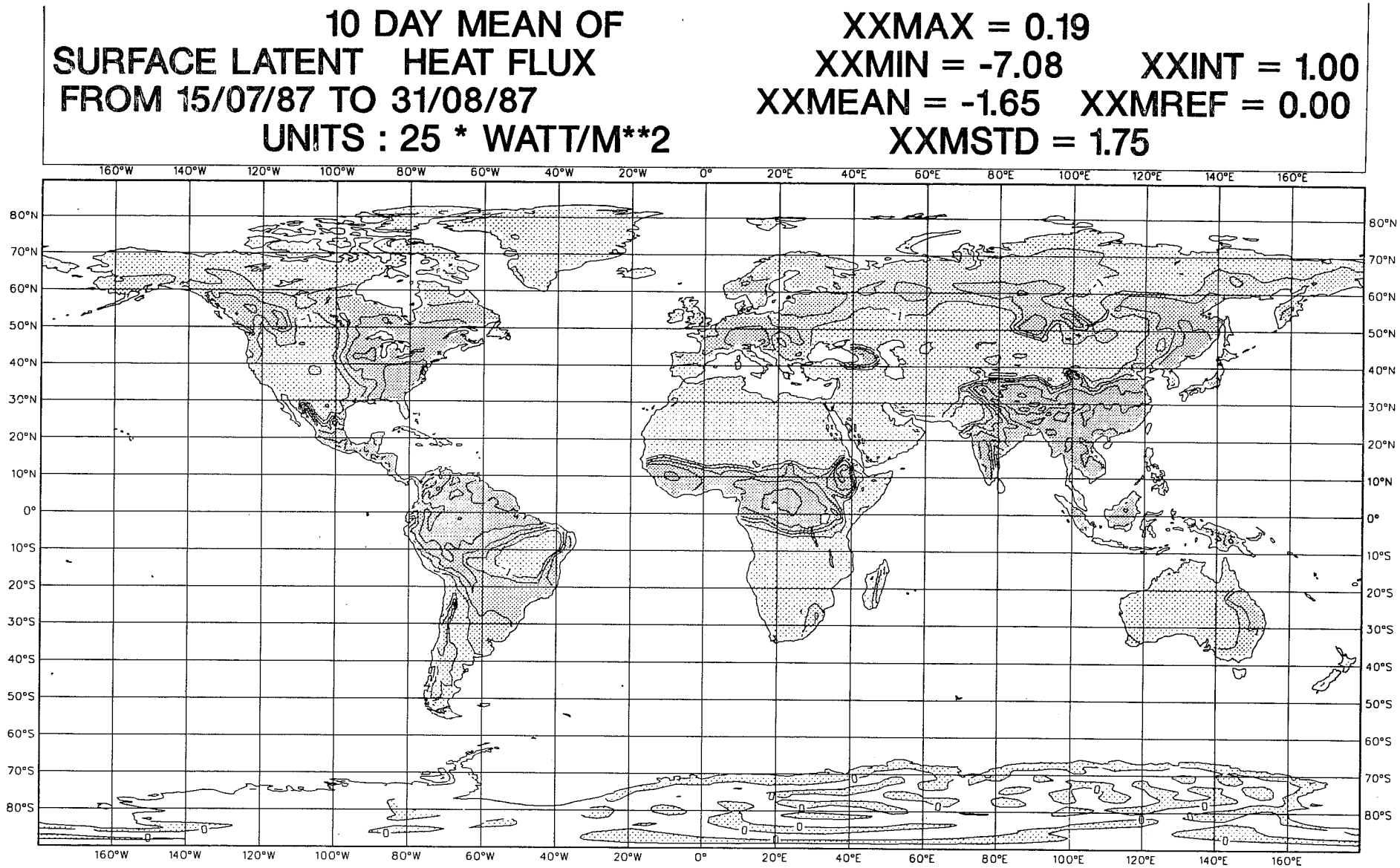

Fig. 7 b) Same as Fig.7a but for the period 15/07/87 to 31/08/87 (CY29 scheme used)

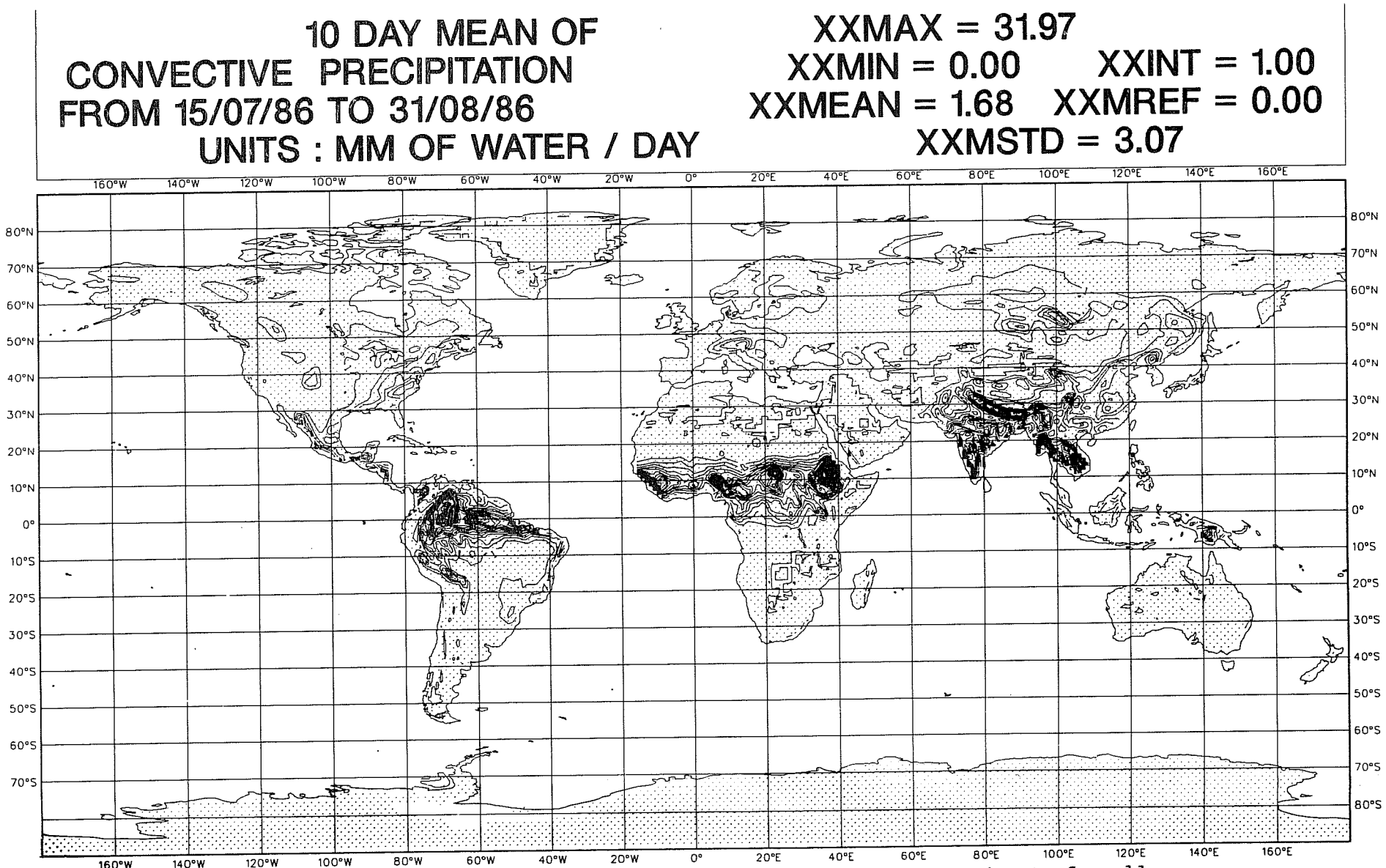

Fig. 8 a) 10 day mean of convective precipitation over the continents for all forecasts from 15/07/86 to 31/08/86 (CY28 scheme used).

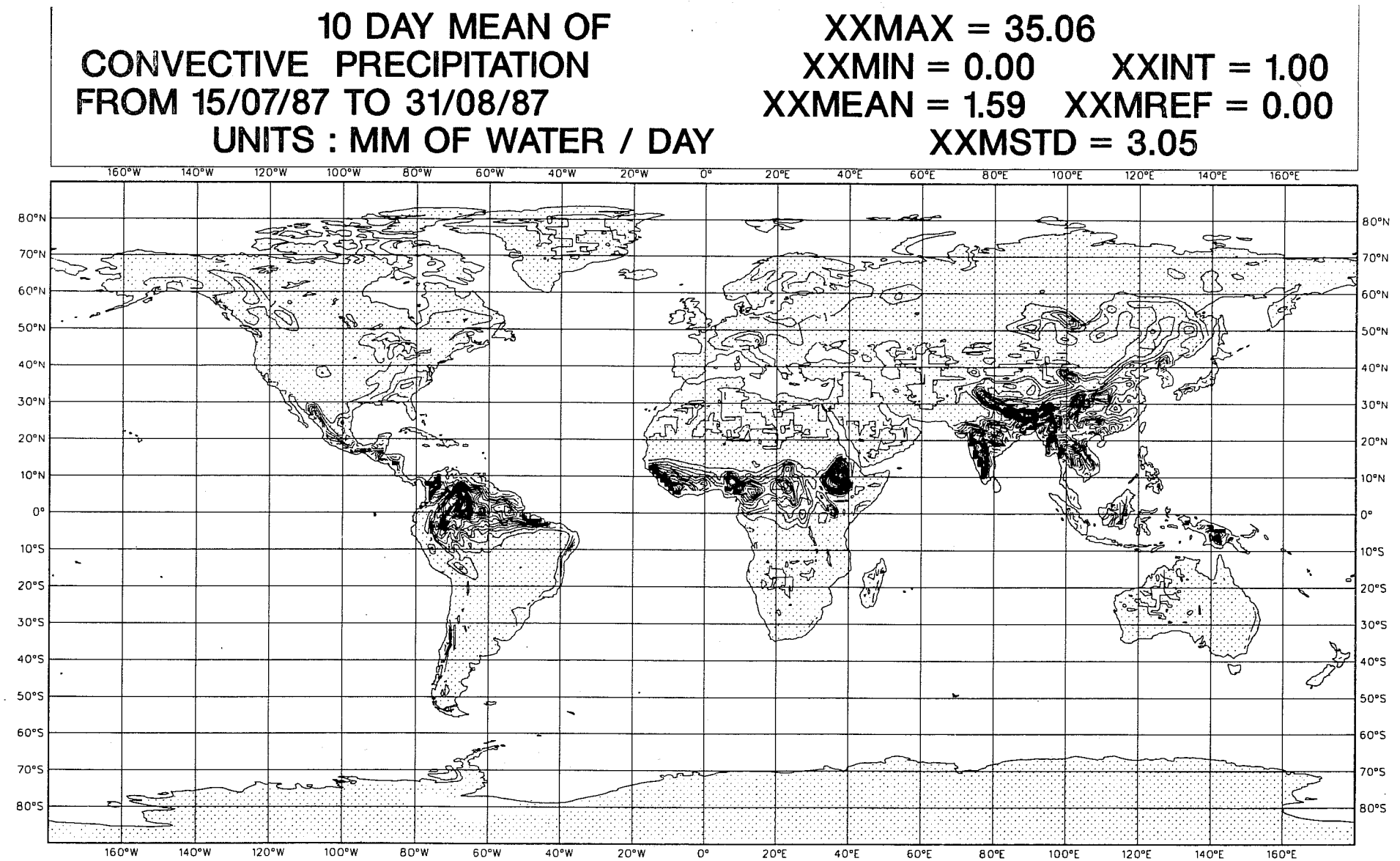

Fig. 8 b) Same as Fig. 8a) but for the period 15/07/87 to 31/08/87 (CY29 scheme used).

same information but for the latent heat flux and the convective precipitation respectively. Mean values are shown in Table 4.

Table 4

	10 day mean sensible heat flux ($W.m^{-2}$)	10 day mean latent heat flux ($W.m^{-2}$)	10 day mean convective precipitation (mm/day)
1986 CY28	35.5	49.0	1.68
1987 CY29	41.5	41.2	1.59

Mean 10 day surface fluxes averaged over the period 15 July to 31 August for the 10 day forecasts run in 1986 and 1987

The remarks made for the parallel runs apply for this longer period. The figures give more insight on the location where the revision has the strongest impact: the reduction of the moisture flux is clear over Brazil, over Africa where a marked narrowing of the evaporating band is seen as well as a shift of the limit of the desert towards the equator in both hemisphere. The modifications of the convective precipitation are strongly correlated in space with those of the evaporation.

Objective scores of the forecasts in the northern hemisphere have not exhibited any interpretable change associated with the revision.

2.4 Modifications of the scheme in response to operational assessment

Diagnostic studies have been carried out in order to document some specific aspects of the model forecasts, generally in response to some failure to capture actual features of the surface state. In this section, the modifications of CY29 in response to the compilation of those diagnostics between April and October 1987 are summarized and briefly discussed. They will be referred to as the CY30 scheme.

First h and R's, as mentined in 2.3 in CY29, were modified to the following expressions:

$$h = 0.5\,[1-\cos(\pi \frac{W_s}{W_{cap}})] \qquad (35)$$

$$R_s = 0.15; \qquad R_d = 0.70; \qquad R_{cl} = 0.15 \qquad (36)$$

Both modifications corrected for the use of too extreme values.

Secondly, a new physical process was added: the shading effect of the canopy. The canopy intercepts precipitation, it also interacts with the solar radiation and decreases the amount of short wave radiation reaching the ground surface. This results in reduced diurnal cycles of soil temperatures in vegetated areas. To simulate this, the thermal diffusivity κ, in Eqs.1 and 2, was modified as follows:

$$\kappa = \begin{cases} 1. - 05\, C_v\, \kappa & \text{if PAR} > 0 \\ \kappa & \text{if PAR} < 0 \end{cases} \qquad (37)$$

This forces the short wave radiation input to be converted to sensible and latent heat flux at the expense of the heat flux inside the ground. This modification leads to a higher surface daytime temperature and smaller diurnal cycle amplitude of the temperature of the intermediate reservoir.

Recent results suggest the need for a reduction of the control by the climate reservoir, and even the exclusion of any root uptake in the deepest reservoir, which can be detrimental in simulating persisting drought conditions. Because the root uptake in this reservoir does not involve soil moisture depletion, the scheme can maintain the transpiration at unrealistically high values. A possible remedy is to change the root profile in order to confine the root extraction to the two top interactive reservoirs. Fig.9 shows the impact of such a change after 6 days of integration in a region (the United States) where the initial values of the two top soil layers are close to the permanent wilting point. Differences of surface temperatures up to 6 degrees can be obtained. A much faster drying of the surface is also clear.

The failure of the scheme to simulate the temperature regimes of some specific areas, like Scandinavia, also suggests that the canopy resistance has to be defined in accordance with the properties of the local vegetation. (The saturation moisture stress is certainly very efficient in reducing the plant transpiration in this area of coniferous forest).

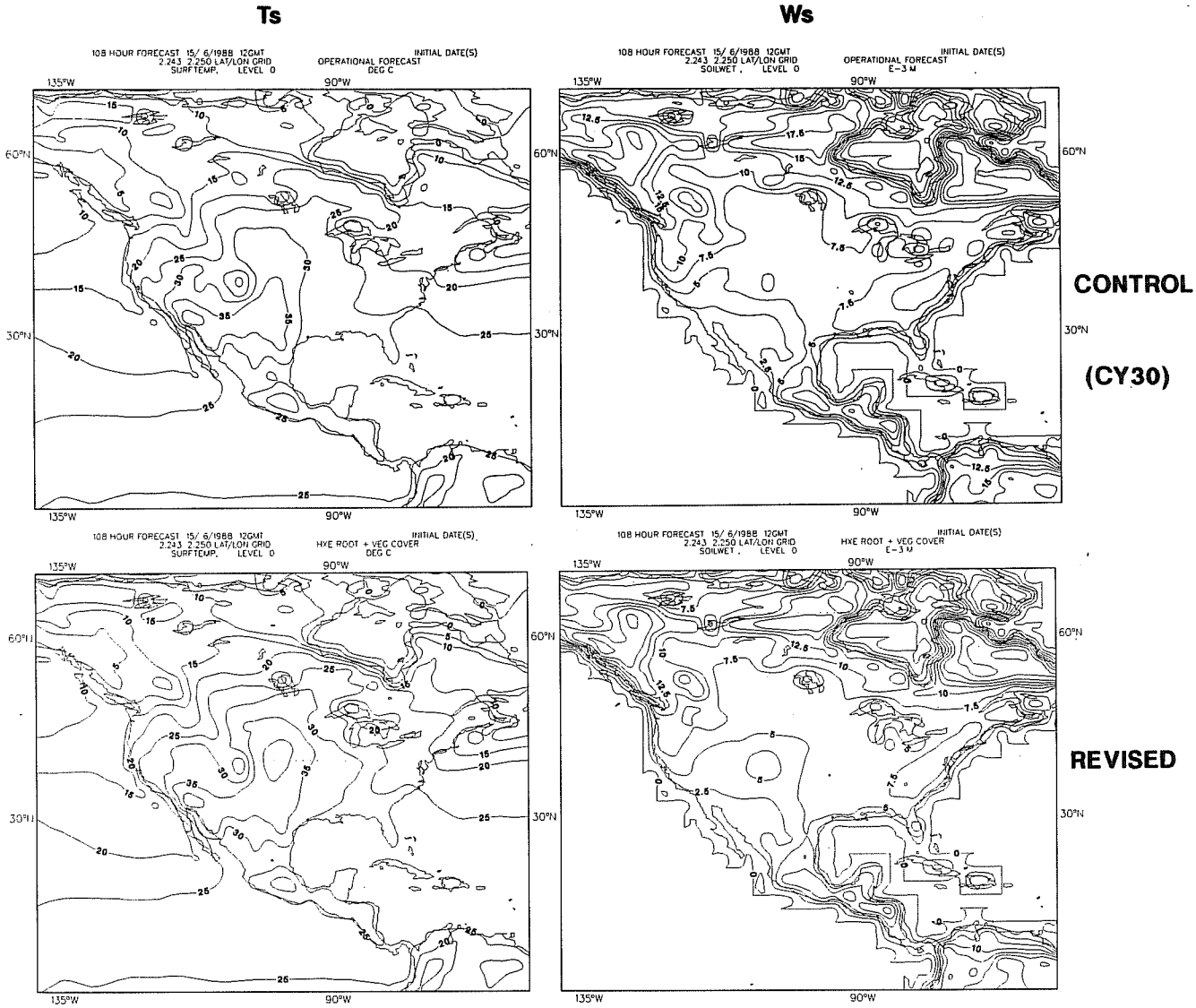

Fig. 9 Comparison of surface temperature Ts (left) and surface soil wetness Ws (right) at Day 5 of a T106 10 day forecast (initial date: 15/06/88) between the current CY30 operational (control/top) and the revised (revised/bottom) surface schemes over the United States (see text 2.4).

The average Bowen ratio in all these runs is much smaller than the V and D estimated one. The surface scheme can easily be tuned to give a more correct value by increasing the stomatal resistance, changing the root profile, modifying the wilting point value, etc... Runs with a revised radiation scheme giving more short wave radiation available at the surface show large variations of the Bowen ratio which becomes very close to accepted estimates (J.J. Morcrette and M. Miller, personal communication).

3. THE TREATMENT OF SNOW IN THE ECMWF MODEL AND ITS EVOLUTION

3.1 Description of the evolution of the snow treatment

Snow has an impact not only on the diurnal evolution of surface temperatures and turbulent fluxes locally but also on the tropospheric flow pattern if it persists for several weeks or months over a large area. It has a feedback on the atmospheric processes through the modification of surface fluxes.

The major and immediate effect of snow is to change the albedo of natural surfaces. This is generally accounted for in numerical models, but an accurate dependence of the surface albedo with respect to snow is difficult to formulate. Snow age and density, interaction with vegetation and fractional snow cover can be taken into account in many ways. In the ECMWF model, the albedo obeys the following empirical formula:

$$\alpha = \alpha_{BG} + (\alpha_{Sn} - \alpha_{BG})\, Sn/(Sn + Sn^*) \qquad (38)$$

where α_{BG} is the geographically variable background albedo, α_{Sn} the albedo of snow, Sn the snow depth and Sn* a critical value. Numerical values are:

$$\alpha_{Sn} = 0.8$$

$$Sn^* = 0.01 \text{ m} \qquad (39)$$

The albedo for the solar parallel flux is modified consistently. No spectral effects are parametrized. On the other hand, the emissivity is not modified by snow. This parametrization has been unchanged since the beginning of the operational use of the spectral model (1983).

The evolution of the snow depth follows:

$$\frac{\partial Sn}{\partial t} = \frac{P_s + C_{Sn} \cdot E_{snow} - M_{Sn}}{\rho_{H_2O}} \qquad (40)$$

where P_s is the precipitation as snow, E_{snow} the evaporation/dew flux over the snow (cf Eq.9) and M_{Sn} the flux of water due to snow melting. The evolution of the treatment of snow has mainly concerned the computation of soil temperatures (since the operational modifications have been implemented in combination with the changes described in paragraph 2, references to CY28, CY29 and CY30 are also relevant for describing the history of the snow treatment and is adopted in the remaining text).

Beside the albedo effect which affects the net radiation available at the surface and the term F in Eq.1, the impact of snow on soil temperatures is accounted for in two steps: firstly, provisional soil temperatures are computed using Eqs.1 and 2, and the possibility of having snow melt is considered; secondly, soil temperatures are updated, the amount of water produced by the melting is subtracted from the snow depth and enters the soil wetness computation.

In the CY28 scheme, Eqs.1 and 2 were used without any modifications in connection with snow covering the ground. Calling $\tilde{T}_s$ the surface temperature computed after integration of Eq.1 over $2\Delta t$, snow melt occurs if $\tilde{T}_s$ is greater than T_o, the melting point temperature ($T_o = 273.16$ K). The amount of snow which can be melted is then given by:

$$\Delta Sn = \min \left[\tilde{Sn}, \frac{C.\, D_1}{L_f\ \rho_{H_2O}} (\tilde{T}_s - T_o) \right] \qquad (41)$$

where L_f is the latent heat of fusion and $\tilde{Sn}$ is the provisional snow depth after solving Eq.40 for $M_{Sn} = 0$.

The final surface temperature is equal to:

$$T_s = \tilde{T}_s - \frac{\Delta Sn\ L_f \cdot \rho_{H_2O}}{C.\, D_1} \qquad (42)$$

The flux of water provided by the snow melt and entering Eqs.3 and 40 is:

$$M_{Sn} = (\Delta Sn/2\Delta t).\ \rho_{H_2O} \qquad (43)$$

The physical interpretation of this scheme is that energy is borrowed from the snow covered ground, transferred by conduction to the snow pack where it is converted in heat of fusion.

This scheme is clearly very simple and has a poor physical basis. Furthermore it does not give satisfactory results in simulating the surface temperature over persistent snow packs or during melting episodes. The most noticeable defects are too weak a diurnal cycle of surface temperature of snow packs for clear sky conditions and too cold surface temperatures during snow melting episodes. The former can be mainly attributed to inappropriate physical coefficients in Eqs.1 and 2, the latter being easily traced back to Eq.42 since surface temperatures T_s can only start to be greater than T_o when all the snow has melted (T_s is an areal mean surface temperature; in a grid box with fractional snow cover, T_s must represent somehow an area weighted mean of the snow covered and the snow free parts of the box. Under melting conditions, it is reasonable to assume that the surface temperature of snow is T_o but that the surface temperature of snow free soils is greater than T_o, leading to a final T_s above the melting point).

CY29 scheme addresses the first questionable point. Snow is not transparent to radiation and has its own thermal properties. Ideally one would like to have coupled equations to compute both ground and snow temperatures. CY29 scheme by-passes this by using the following equations:

$$\frac{\partial T_s}{\partial t} = \frac{F}{C^*.\ D_1} + 2\kappa^* \frac{(T_d - T_s)}{D_1.(D_1+D_2)} \qquad (44)$$

$$\frac{\partial T_d}{\partial t} = 2\kappa^* \frac{(T_s - T_d)}{D_2.(D_1+D_2)} + \kappa \frac{(T_{cl} - T_d)}{D_2.D_2} \qquad (45)$$

where:

$$C^* = C(1-C^*_{Sn}) + C_i\, C^*_{Sn} \qquad (46)$$

$$\kappa^* = [(1-C^*_{Sn}) + a.C^*_{Sn}]\ \kappa \qquad (47)$$

$$C_i = 2.09\ 10^6\ J.m^{-3}.K^{-1}; \quad a=0.3; \quad C^*_{Sn} = \min(1, Sn/D_1)$$

The key idea of this modification is to improve the simulation of surface temperature of persistent thick snow packs, which cover the ground completely. It is not an attempt to tackle the fresh snow case, but to represent old packed snow. For this type of snow, data indicate that, for a snow density of 0.25 against water, the influence of the surface diurnal cycle concerns the topmost 20 to 30 centimetres of snow (equivalent to snow depths Sn between 5 and 7.25 cm. For convenience, D1, which is equal to 7 cm, is kept as scaling parameter). Fig.10 shows a geometric interpretation of the CY29 scheme.

The specification of a in Eq.47 is empirical. It represents exchanges both between ground/ground slabs and snow/ground slabs. It can be seen that if $Sn > D_1$, T_d still represents a ground temperature. Lower thermal diffusivities in the CY29 than in the CY28 scheme favour larger diurnal amplitudes of surface temperature, generally having lower mean daily surface temperatures since lower values of heat capacity enhance the contribution of nightime radiative cooling compared to daytime insolation warming because of the asymmetry of day/night at the latitudes and periods of the year for which this scheme works.

Snow melting in CY29 is similar to CY28, except that Eq.46 is also used to define the heat capacity in Eqs.41 and 42. But T_s cannot be higher than T_o unless the snow is completely melted.

The impact of the CY29 snow changes on the model climate is seen in the northern hemisphere wintertime runs reported in 2.3.2. The mean surface temperatures of CY28 and CY29 runs are very close, while the temperature of the intermediate layer is warmer in CY29 than in CY28 runs. T_s is a mean between warmer snow free areas and colder snow covered soils. Lower values of thermal diffusivity over soil covered ground decreases the influence of the surface cooling on T_d.

The CY30 scheme keeps Eqs.44 and 45 of the CY29 scheme, but the possibility of snow melt is treated differently. There are two main guiding ideas in the CY30 scheme. First, radiation and sensible heat (very significant under foehn conditions for instance) fluxes help to melt the upper part of a snow pack. However the water has to drip inside the snow mantle before reaching the ground and contributing to modify the surface soil wetness; it must not refreeze inside the snow pack. Thus it is possible to have surface melting conditions but no variation of the total snow/ice depth. This will be called "surface" melting. Secondly, snow can melt by heat conduction over a soil which temperature is above T_o by borrowing energy from the soil and converting it in heat of fusion (this is the scenario of CY28 and CY29 schemes). But the energy is borrowed from the ground directly underneath and not from the whole ground surface layer in case of $C^*_{Sn} < 1$.

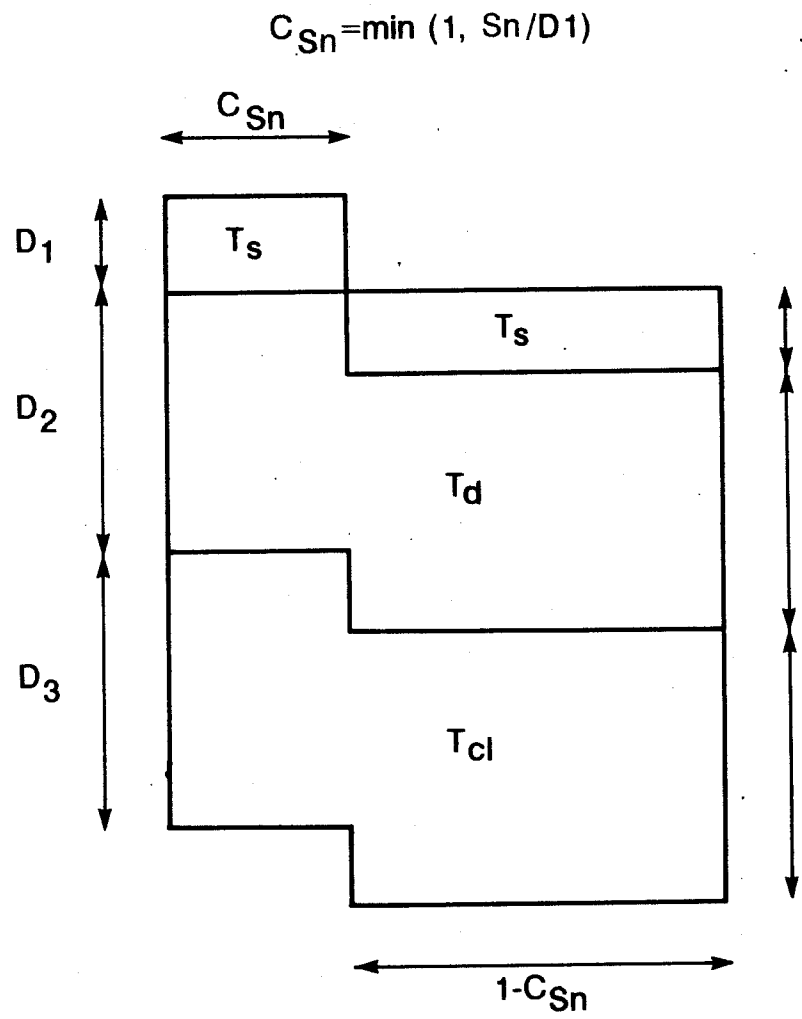

Fig. 10 Geometric interpretation of the snow scheme treatment (see text 3.1).

This will be called "deep" melting.

CY30 scheme works as follows:

i) Eqs.44 and 45 provide provisional temperatures $\tilde{T}_s$ and $\tilde{T}_d$, Eq.40 a provisional snow depth .

ii) If $\tilde{T}_s < T_o$, provisional values become final values.

If $\tilde{T}_s > T_o$, it is assumed that "surface" melting conditions have been met.

$\tilde{T}_s$ is thus an area weighted temperature of a depth D1 of snow at T_o covering C^*_{Sn} of the grid and a depth D_1 of snow free ground (fraction (1 - C^*_{Sn}) of the grid) at some temperature T1 greater than T_o given by:

$$[C^*_{Sn} C_i + (1-C^*_{Sn}) C] \tilde{T}_s = C^*_{Sn} . C_i.T_o + (1-C^*_{Sn}).C.T_1 \quad (48)$$

The mean temperature of the ground slab of depth D1 for the whole grid is given by:

$$T_e = \tilde{T}_s + C^*_{Sn} [(\tilde{T}_d - T_s) + \frac{C_i}{C} (\tilde{T}_s - T_o)] \quad (49)$$

iii) If $T_e < T_o$, no deep melting occurs. It is then assumed that the temperature of the depth D1 of snow is T_o since there is surface melting and that the energy transported inside the snow pack by the refreezing water is ultimately gained by the soil slab of depth D_1 just below the snow pack. Defining T_{d1} and ΔT_d by:

$$\Delta T_d = \frac{C_i}{C} (\tilde{T}_s - T_o) = T_{d1} - \tilde{T}_d \quad (50)$$

the final soil temperatures read:

$$T_s = \frac{C^*_{Sn}.C_i . T_o + (1-C^*_{Sn}).C. \tilde{T}_s}{C^*_{Sn}. C_i +(1-C^*_{Sn}). C} \quad (51)$$

$$T_d = \bar{T}_d + \frac{D_1}{D_2} C^*_{Sn} \Delta T_d \qquad (52)$$

If $T_e > T_o$, deep melting occurs. The amount

$$\Delta Sn = \min [Sn, C^*_{Sn} \frac{C. D_1}{L_f \rho_{H_2O}} (T_e - T0)] \qquad (53)$$

is melt, which corresponds to the snow cover decrease:

$$\Delta C_{Sn} = C^*_{Sn} - \min [1 (Sn-\Delta Sn)/D_1] \qquad (54)$$

Calculations are then similar to Eqs.51 and 52, but with $T_{d1} = T_o$ and the change of snow cover taken into account. Final soil temperatures read:

$$T_s = \frac{(C^*_{Sn}-\Delta C_{Sn}). C_i . T_o + \Delta C_{Sn}. C. T_o + (1-C^*_{Sn}) T_e}{(C^*_{Sn}-\Delta C_{Sn}) . C_i + [1 - (C^*_{Sn} - \Delta C_{Sn})] . C} \qquad (55)$$

$$T_d = \bar{T}_d + (C^*_{Sn} - \Delta C_{Sn}). \frac{D_1}{D_2} (T_o - \bar{T}_d) \qquad (56)$$

In contrast with CY28 or CY29, the CY30 scheme allows surface temperatures above T_o even when there is still snow covering the ground. Fig.11 illustrates this feature in showing snow depth and surface temperature during a snow melting episode produced by schemes CY29 and CY30 in a simple test. An atmospheric forcing (F in Eqs.1 and 44) is imposed at the surface of a soil column. Initial conditions are:

$$T_s = T_d = T_{cl} = T_o$$

The CY29 scheme generates a sudden (and unrealistic) change of surface temperature as soon as Sn = 0, whilst daytime surface temperature exhibit a continuous and smooth evolution from day to day using CY30.

3.2 Comments on the operational implementation of the schemes

The snow depth Sn is analysed using snow depth reports provided by synoptic observing stations, or temperature and precipitation reports (ECMWF, 1988). This analysis does not

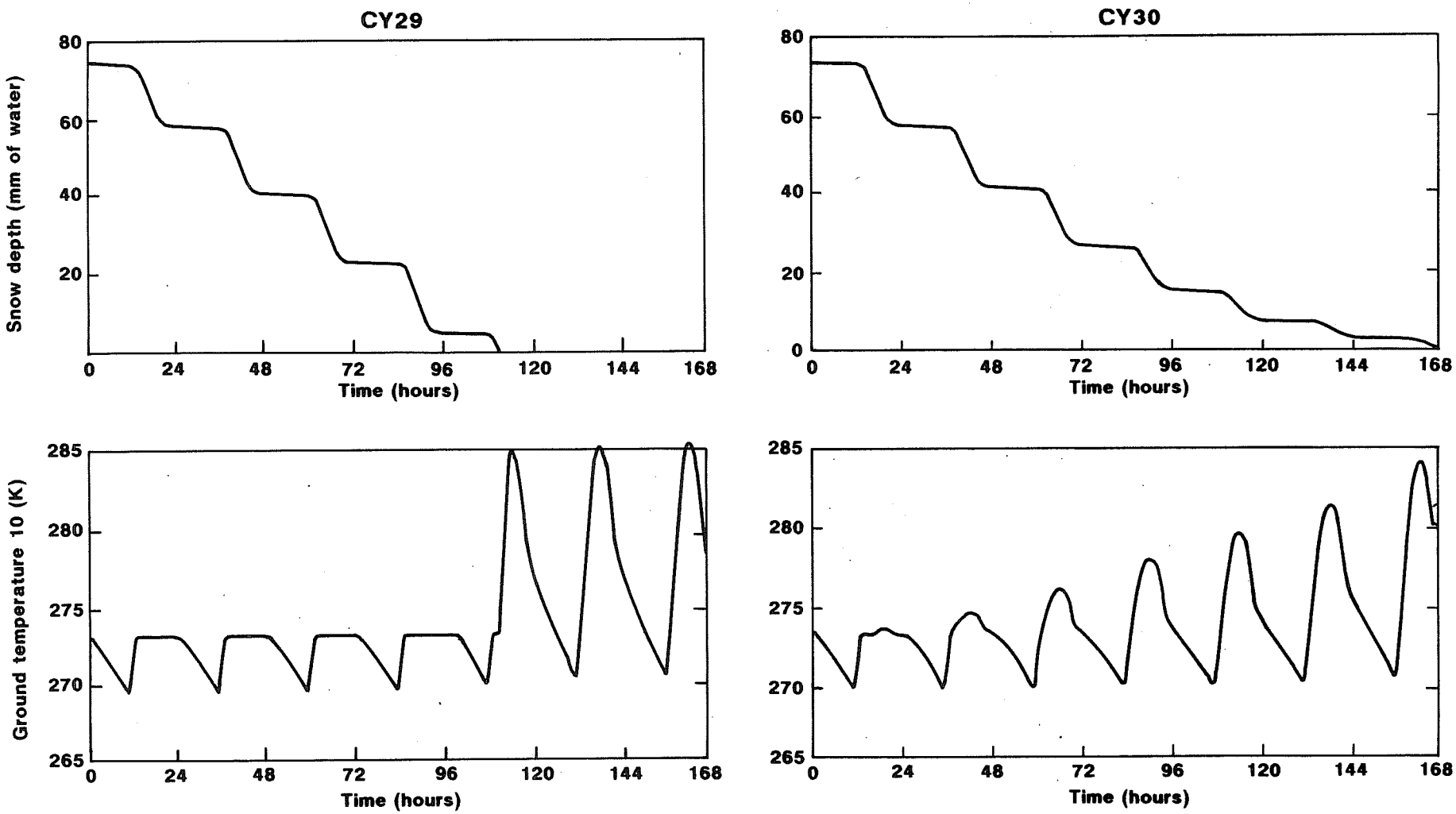

Fig. 11 Surface temperature and snow depth evolution during a snow melt episode with:
Left: CY29 scheme - The energy needed to melt the snow is borrowed from the entire grid box
Right: CY30 scheme - The energy needed to melt the snow is borrowed from the part of the grid box covered by the snow.

make use of first guess model generated values. Though some corrections are made to the first guess surface temperature to ensure some consistency with the snow scheme used in the forecast (D. Vasiljevic, personal communication), the initial state of snow on one hand and of soil temperature on the other hand are obtained via basically independent approaches. It is thus difficult to evaluate the quality of the snow scheme through its performance during the forecast since the initial state may already be largely in error. This may be the case especially in regions of poor data coverage or regions which do not report snow or precipitation observations on the GTS: in these cases the analysis assigns climate values of snow depth which can be totally wrong compared to the actual situation. However, by and large, surface temperature over snow produced by CY29 and CY30 schemes are generally in agreement with observations over permanent thick snow packs. Most problems are connected to partially snow covered grounds, snow packs under snow free canopies and melting conditions (see B. Strauss' paper). Scientists outside ECMWF using the ECMWF model for climate studies also reported that the snow generated by the model during winters stays generally too long during springs because the albedo formulation (Eq.38) biases strongly the net radiation at the ground.

A simple experiment helps to illustrate the problems still pending. As for the experiment illustrated in Fig.12 , a soil column experiences an imposed atmospheric forcing (no diurnal cycle is included):

$$F = (2\text{-alb})\, F_1 \; ; \; F_1 = 30 W.m^{-2}$$

The albedo is computed using Eq.38 with $\alpha_{B.G} = 0.2$. The initial values are:

$$T_s = T_d = T_o - 10\,(K) \; ; \; Sn = 0.15\ m$$

Experiments are carried out for three different values of the deep climate temperature T_{cl}: -5°C, 0°C and 5°C. For each T_{cl}, CY28, CY29 and CY30 schemes are run. A fourth experiment labelled ALB on Fig.12 corresponds to the CY30 scheme but with the modified Eq.38 :

$$\alpha = \alpha_{B.G} + (\alpha^*_{Sn} - \alpha_{B.G}) \frac{Sn}{Sn + Sn^*}$$

with:

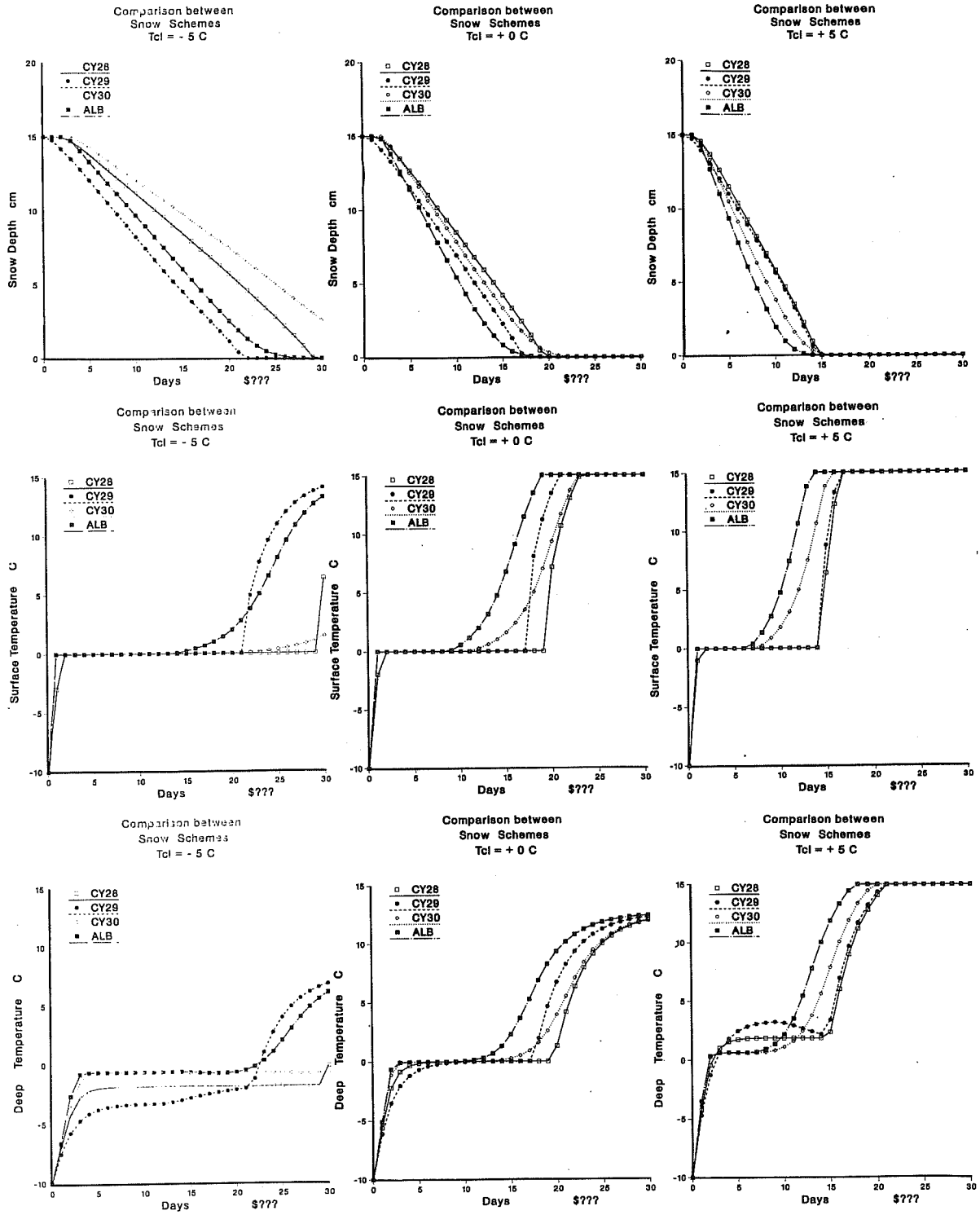

Fig. 12 Simulation of snow melting and surface temperature with various surface scheme as a function of the climate deep temperature Tcl (see text 3.2).

$$\alpha^*_{Sn} = \begin{cases} 0.8 & \text{if } T_s < T_o \\ 0.4 & \text{if } T_s \geq T_o \end{cases}$$

Results clearly indicate that the way a snow pack evolves is as much dependent on the physics involved in the snow parametrization as on values of either "external" fields like the soil deep climate temperature or more "internal" parameters like the snow albedo.

4. CONCLUSIONS

The evolution of the surface schemes used in the operational ECMWF model has been described. The main reasons for initiating some work on this aspect of the physical package were motivated by:

- direct and indirect indications that surface evaporation and the diurnal cycle over land were not adequately represented,

- the possibility of implementing more physically sound schemes,

- the need for revising the analysis of surface parameters,

- the prospect of using more appropriate soil characteristics either based on existing or future datasets or derived from routine observations.

For the time being, most of the work which has led to modifications in the ECMWF model has concerned the revision of the parametrization of surface moisture fluxes over land and the treatment of snow. It has been shown that important aspects of the surface budgets like the Bowen ratio, the ratio between precipitation over the oceans and the continents can be improved globally without a lot of refinement in the specification of vegetation characteristics or soil properties. However, remaining failures of the forecasting system (data assimilation + forecast) to follow the actual surface state evolution is generally traced back to inadequate surface properties or too strong an influence of the soil deep climate.

The change from CY28 to CY30 has not provided a major improvement of the forecast at the synoptic scales, despite positive impact on the surface weather elements. Ongoing research on other aspects of the model (radiation, convection) indicates that the performance of any surface scheme is still very much dependent on the quality of surface fluxes like the net radiation or the precipitation. Nevertheless the possibility of using deterministic forecasts at ranges up to two weeks will demand more and more attention to surface processes, the importance of which increases with the forecast range.

Future work should concentrate on improving the specification of surface variables. This will involve major revision in the analysis of surface variables (use of 3-D variational assimilation methods for instance which make use of routine measurements like 2m temperature or surface precipitation possible in a way consistent with the model physics) and effort in deriving surface properties (soil + vegetation) from existing or future datasets and satellite measurements.

References

Blondin, C., 1986 : Treatment of land-surface properties in the ECMWF model. ISLSCP - Parameterisation of Land-surface Characteristics; Use of Satellite Data in Climate Studies; First Results of ISLSCP. Rome, Italy, 2-6 December 1985, 53-60.

Blondin, C. and H. Böttger, 1987: The surface and sub-surface parametrization scheme in the ECMWF forecasting system: Revision and operational assessment of weather elements. ECMWF, Res. Dept. Tech. Memo., No. 135, 20 pp + 33 Figs.

Blondin, C., 1988: Parametrization of land-surface processes in numerical weather prediction. Measurements and Parametrization of Land-surface Evaporation Fluxes, Banyuls, France, 10-21 October 1988 (to be published in WMO/WGNE series).

Budyko, M.I., 1956: Heat balance at the earth's surface. Gidrometeoizdat, Leningrad, 225 pp. (in Russian).

Clapp, R.B., and G.M. Hornberger, 1978: Empirical equations for some soil hydraulic properties. Water. Resources Res., 14, 601-604.

Deardorff, J.W., 1978: Efficient prediction of ground surface temperature and moisture, with inclusion of a layer of vegetation. J.Geoph.Res., 83 (C4), 1889-1903.

Dickinson, R.E., A. Henderson-Sellers, P.J. Kennedy, and M.F. Wilson, 1986: Biosphere/Atmosphere Transfer Scheme (BATS) for the NCAR Community Climate Model. NCAR Tech. Note, TNXXX, NCAR, Boulder, CO, 80307.

ECMWF, 1984: ECMWF data assimilation - Scientific documentation. Research manual 1, original version (edited by Lönnberg and Shaw).

ECMWF, 1988: ECMWF data assimilation - Scientific documentation. Research manual 1, revision 2 (edited by Lönnberg).

Louis, J.F., 1979: A parametric model of vertical eddy fluxes in the atmosphere. Bound. Layer. Meteor., 17, 187-202.

Louis, J.F., Tiedtke, M., and Geleyn, J.F., 1982: A short history of the PBL parametrization at ECMWF. ECMWF Workshop on Planetary Boundary Layer Parametrization. Reading, United Kingdom, 25-27 November 1981, 59-80.

Mintz, Y., 1984: The sensitivity of numerically simulated climates to land-surface conditions. The Global Climate, J. Houghton, Ed., Cambridge University Press, 79-105.

Monteith, J.L., 1965: Evaporation and environment. Symp. Soc. Exptl. Biol., 19, Swansea, 8-12 September 1964, 205-234.

Rowntree, P.R. and J.A. Bolton, 1983: Simulation of the atmospheric response to soil moisture anomalies over Europe. Quart. J. R. Met. Soc., 109, 501-526.

Sellers, P.J., 1985: Canopy reflectance, photosynthesis and transpiration. Contractor Rapport 177822, NASA/GSFC, Greenbelt, MD 20771, U.S.A.

Sellers, P.J., Y. Mintz., Y.C. Sud, and A. Dalcher, 1986: A Simple Biosphere model (SiB) for use within general circulation models. J. Atmos. Sci., 43, 505-531.

Verstraete, M.M. and R.E. Dickinson, 1986: Modelling surface processes in atmospheric general circulation models. Ann.Geophysic., 4, B, 4, 357-364.

Wilson, M.F., and A. Henderson-Sellers, 1985: Cover and soil datasets for use in general circulation climate models. J. Climatol., 5, 119-143.